



# Brine migration along vertical pathways due to CO<sub>2</sub> injection - a simulated case study in the North German Basin with stakeholder involvement

Alexander Kissinger<sup>1</sup>, Vera Noack<sup>2</sup>, Stefan Knopf<sup>2</sup>, Wilfried Konrad<sup>3</sup>, Dirk Scheer<sup>3</sup>, and Holger Class<sup>1</sup>

<sup>1</sup>Department of Hydromechanics and Modelling of Hydrosystems, University Stuttgart, Pfaffenwaldring 61, 70569 Stuttgart, Germany

<sup>2</sup>Bundesanstalt für Geowissenschaften und Rohstoffe (BGR), Stilleweg 2, 30655 Hannover

<sup>3</sup>DIALOGIK, Lerchenstraße 22, 70176 Stuttgart, Germany

*Correspondence to:* Alexander Kissinger (alexander.kissinger@iws.uni-stuttgart.de)

**Abstract.** Brine migration into potential drinking water aquifers due to the injection of CO<sub>2</sub> into deep saline aquifers is one of the potential hazards associated with the Carbon Capture and Storage technology (CCS). Thus, in any site selection process, an important criterion should be the evaluation of brine migration resulting from the injection. We follow an interdisciplinary approach using participatory modeling to incorporate stakeholder opinion at an early stage in order to discuss and evaluate model conception and relevant scenarios for brine migration. The basis for this approach is a realistic (but not real) on-shore site in the North German Basin with characteristic geological features for that region. Our model fully couples flow in shallow and in deep saline aquifers including variable-density transport of salt and a realistic description of the top surface boundary conditions with groundwater recharge and rivers. We investigate different scenarios to identify relevant system components. Further, different model simplifications are compared and discussed with respect to the relevant physical processes and the expected data availability, i.e. to find a model as complex as necessary and as simple as possible. It becomes clear that the initial salt distribution plays a key role as to where noticeable concentration changes may occur. Also the boundary conditions are important for determining the amount of vertically displaced brine. Simplifications in the model setup, such as neglecting variable-density flow or simplifying the complex geometry may prove valid options given sparse data availability.

## 1 Introduction

Current research for capture and storage (CCS) is at a stage where the transition from pilot to large-scale demonstration projects appears overdue, at least if the potential for this technology as an option for mitigating global climate change shall be assessed on a climate-relevant scale. Although successful storage of CO<sub>2</sub> has been shown, for example, at the Ketzin (Martens et al., 2012) and Sleipner site (Skalmeraas, 2014), further large-scale demonstration projects are needed to improve the understanding of a safe and efficient storage (IEA, 2013). The identification of possible storage sites generally involves a multi-stage process, where different criteria have to be evaluated, such as storage capacity, storage efficiency, technical and economical feasibility as well as criteria regarding the safety of the storage.

The injection of super-critical CO<sub>2</sub> into deep saline aquifers inevitably leads to the displacement of resident brine. Hazardous



situations may arise if brine migrates vertically through discontinuities like permeable fault zones or abandoned wells into shallow aquifer systems, where the brine may contaminate drinking water. Salt concentrations at a drinking water production well should not rise above the regulatory limits and eventually lead to a shutdown of production. In the last decade, there has been much research in the field of brine migration, and new insights were gained through means of large-scale numerical and analytical models. The extent of pressure propagation was already the subject of several simulation studies. Model predictions have shown that the area for potential brine migration to occur is much larger than the actual extent of a CO<sub>2</sub>-plume (2-8 km), as elevated pressures are predicted up to 100 km from the injection well (Birkholzer et al., 2009; Birkholzer and Zhou, 2009; Schäfer et al., 2011). Schäfer et al. (2011) performed simulations in a realistic geological system consisting of aquifer and barrier formations bounded by a sealing fault zone. Birkholzer et al. (2009) considered a generic geometry in a multi-layered system consisting of a sequence of aquifers and aquitards, thereby investigating both lateral and vertical pressure propagation. They conclude that leakage across aquitards needs to be considered for realistic pressure propagation, if the sealing aquitards have a permeability higher than  $1 \cdot 10^{-18} \text{ m}^2$ . However, they do not expect significant damage due to vertical brine migration unless vertical pathways such as permeable fault zones or abandoned wells exist where focused leakage may occur. More recent studies focus on the simplification of the simulation tools for quantifying brine migration and developing pressure management tools. Brine leakage through abandoned wells was investigated in Celia et al. (2011) using a semi-analytical model described in Celia and Nordbotten (2009) and Nordbotten et al. (2009). A comparison of models of varying complexity on the basin scale with multiple injection wells was conducted by Huang et al. (2014). They concluded that single-phase numerical models are sufficient for predicting basin scale pressure response. Analytical and semi-analytical solutions depending on superposition of solutions in time and space may not be accurate enough as the variability of formation properties (heterogeneity and anisotropy) cannot be captured. Cihan et al. (2011) developed an analytical model capable of handling multi-layered systems considering diffuse leakage (through aquitards) and focused leakage (abandoned well and fault zones). The same analytical model is also applied in Birkholzer et al. (2012), where pressure management strategies are compared. Zeidouni (2012) presented an analytical model for determining brine flow through a permeable fault zone into aquifers separated by impermeable aquitards. This model has a realistic description of the fault zone, as lateral and vertical transmissivity within the fault zone can be assigned independently of each other, thereby allowing a wide range of fault zone configurations. Oldenburg and Rinaldi (2010) set up an idealized numerical model of two aquifers separated by an aquitard with a connecting permeable fault zone. They show that a new hydrostatic equilibrium may establish if salt water is pushed upwards through a fault zone due to an increase in pressure in the lower aquifer. The new equilibrium strongly depends on the salt concentration in the lower aquifer, where low concentrations may lead to continuous upward flow as opposed to high salt concentrations. Tillner et al. (2013) consider brine migration scenarios for a potential storage in northern Germany using a multi-phase (H<sub>2</sub>O and CO<sub>2</sub>) and multi-component (H<sub>2</sub>O, NaCl and CO<sub>2</sub>) model accounting for density differences due to variable salt concentrations. They included several fault zones which can be permeable or impermeable, thereby controlling leakage into overlying aquifers. They conclude that the choice of boundary conditions for the lateral boundary has the highest impact on the observed brine migration, while the results are less sensitive to the fault permeability. The model for the deep subsurface used by Tillner et al. (2013) was further coupled (one-way coupling) to a model comprising more shallow freshwater aquifers (Kempka et al., 2013) using



flow through the fault zones as boundary conditions for the shallow aquifer model. The results indicate that an increase in the salt concentration due to CO<sub>2</sub>-injection is only recognizable in areas already having a naturally elevated salt concentration. Walter et al. (2012, 2013) use a generic multi-layer system with a radially symmetric fault zone surrounding the injection at a certain distance. They also use a multi-phase (H<sub>2</sub>O and CO<sub>2</sub>) and multi-component (H<sub>2</sub>O, NaCl and CO<sub>2</sub>) model to calculate the brine flow into a shallow aquifer. Walter et al. (2012) assume a constant initial salt concentration across the deep layers, and in Walter et al. (2013), they assume a linear salt concentration gradient increasing with depth. The results show that the amount of salt entering the shallow aquifer varies significantly between these two assumptions, with more salt entering in the constant concentration case. Therefore, the calculation of salt transport into shallow aquifers is not only uncertain with respect to boundary conditions and hydrogeological parametrization but also with respect to the initial salt concentration in the system. A number of numerical studies have been conducted modeling large scale heat and salt transport in the North German Basin to determine regional flow fields. Magri et al. (2009a, b) model two-dimensional heat and salt transport near shallow salt structures piercing through a layered aquifer/aquitard system. They argue that topographically-driven flow, gravitational and thermohaline convection are the major mechanisms that lead to solute exchange between deep and shallow layers. Noack et al. (2013) model three-dimensional regional heat transport and find that temperature anomalies occur at hydrogeological windows in the Rupelian clay barrier (barrier between deeper saline and shallower freshwater aquifers) where cooler water from shallow aquifers displaces the warmer formation water. Kaiser et al. (2013) extend this work by including salt transport in their model of the Northeast German Basin.

This study here has its focus on the effect of large-scale brine migration on the groundwater system due to CO<sub>2</sub> injection for a realistic (but not real) geological structure in the North German Basin. The latter is the most relevant region regarding CO<sub>2</sub> storage capacity in Germany (Knopf et al., 2010). The geological model comprises layers from the injection horizon in the deeper saline aquifer up to potential drinking water horizons in the shallow, freshwater aquifers. This includes characteristic geological features of the North German Basin. In contrast to earlier work, for example by Kempka et al. (2013), our model fully couples flow in shallow aquifers with deep saline aquifers considering variable-density flow. Within this system, we investigate the potential for brine migration as required for an early assessment of a multi-stage site identification process. Public acceptance and understanding is a key issue on the way towards realizing such projects. Therefore, it is good practice to involve stakeholders at an early stage during the site identification process (Scheer et al., 2015). Using participatory modeling (PM), we incorporate stakeholder opinion to discuss the geological model setup and relevant scenarios for brine migration, which then feeds back into the geological and numerical modeling process. Following this societal and technical approach, reference is made below to social scientists and geo-modelers when presenting the PM approach. With the term “geo-modelers“ we synthesize the expertise of authors having a background in geology and numerical modeling. In the results section, we analyze different scenarios highlighting relevant system components for brine migration. Furthermore, we test different model simplifications that seem reasonable in the light of sparse data availability and discuss their effect on relevant target variables.

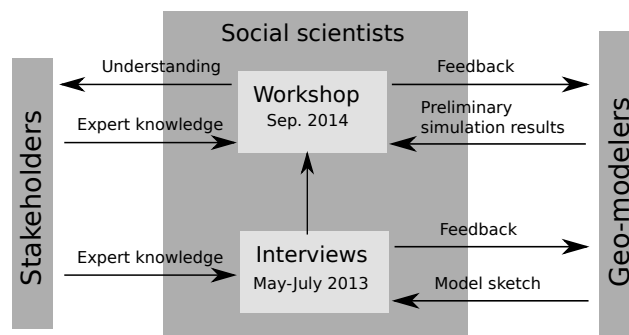


**Figure 1.** The participatory modeling (PM) process.

## 2 Participatory modeling

Any effort in investigating and developing CCS unavoidably touches the social and political sphere and needs to take into account the broader societal debate on possible energy futures. From the very beginning this research on brine migration, as presented here, aimed at involving expert's and stakeholder's knowledge in simulating the impacts of injecting CO<sub>2</sub> into deep saline aquifers. The concept of PM provides a framework for integrating external expertise into producing and deploying conceptual and computer-based models (Bots and Daalen, 2008; Dreyer et al., 2015; Dreyer and Renn, 2011; Röckmann et al., 2012). PM is a generic approach, open for different methods facilitating early expert and stakeholder integration in science development. The involvement exercise undertaken within the modeling of brine migration scenarios made use of two approaches. As a starting point, guideline-based interviews carried out by the social scientists aimed at eliciting expert and stakeholder knowledge and assessments on geological structures and mechanisms impacting CO<sub>2</sub> induced brine migration. The second involvement approach consisted of a stakeholder workshop including the world café deliberation format (Fouché and Light, 2011) and was carried out with the objective of evoking evaluations and judgments on the modeling approach, scenario selection and preliminary simulation results. An overview of the PM process that was carried out is given in Fig. 1.

### 2.1 Technical information for the stakeholders

The main information from the geo-modelers was the introduction of a geological model comprising layers from the injection horizon in the deeper saline aquifer up to potential drinking water horizons in the shallow, freshwater aquifers. Geological data from 3D models of a region in the southwestern German North Sea were used as a database for the construction of a structural model of the deep subsurface (Bombien et al., 2012; Asprión et al., 2013; Kaufmann et al., 2014; Wolf et al., 2014). The region is part of the North German Basin (NGB). Potential reservoir- and barrier rock units of the NGB have been evaluated in recent years (e.g. Reinhold et al. (2011); Jähne-Klingberg et al. (2014)). Accordingly, suitable Permian Upper Rotliegend- and Triassic Middle Buntsandstein reservoir rock units are widely spread across the NGB, thus holding the bulk of subsurface storage potential (Fig. 2). In addition to deeply buried barrier rock units like Permian Zechstein evaporites and Triassic Upper Buntsandstein evaporites and shales, a special focus may be put on the Oligocene Rupelian clay, which forms an important

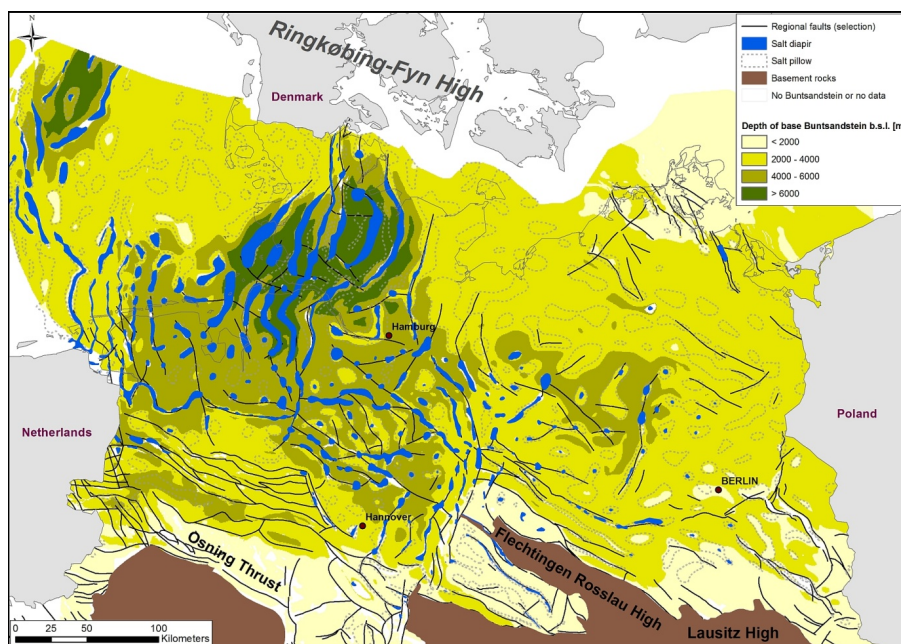


**Figure 2.** Extent and depth of the Buntsandstein group and important structural elements in the North German Basin (depicting data only for the German mainland and the German sectors of the North Sea and the Baltic Sea). Based on Reinhold et al. (2008), Doornenbal and Stevenson (2010), Schulz et al. (2013).

regional hydraulic barrier (in this work referred to as Rupelian clay barrier) between shallow freshwater aquifers and deep saline aquifers in the NGB (Reinhold et al., 2011). Salt tectonics led to the development of ca. 450 salt structures (Reinhold et al., 2008), which have either bent upward (salt pillows) or penetrated the overburden (salt diapirs and salt walls). Thus, many geological structures were formed that may act as traps for the storage of buoyant fluids.

- 5 The database for the construction of the geological model covers depth lines of an elongate anticlinal structure of Mesozoic sediments on top of a salt pillow (Permian Zechstein salt). This dome structure descends gently into a structural low (Syncline). The latter is bordered by an elongate steeply rising salt wall (diapir). For the CO<sub>2</sub> injection scenarios, the dome structure including the injection horizon acts as structural trap, whereas the salt wall forms a natural boundary for displaced brine. Based on these geological features, the geo-modelers constructed a sketch for the guideline-based interviews (Fig. 3). The sketch
- 10 also indicates pathways for brine, such as abandoned wells, fault zones and hydro-geological windows in the Rupelian clay barrier. The assumption of fluid migration via vertical pathways in sediments flanking salt structures is a matter of debate. After LBEG (2012) "the contact zone between salt domes and the CO<sub>2</sub>-sequestration horizon is assumed to be a zone of weakness, similar to geological faults". Such zones of weakness may provide effective vertical migration pathways. To the understanding of the geo-modelers, this could be a possible scenario at shallower depth in the sediments on top of the hanging wall of diapirs
- 15 if recent halokinetic salt movements occur. Based on feedback from the guideline-based interviews and own considerations, several possible migration pathways were included in the geological model, like hydro-geological windows and a fault zone at

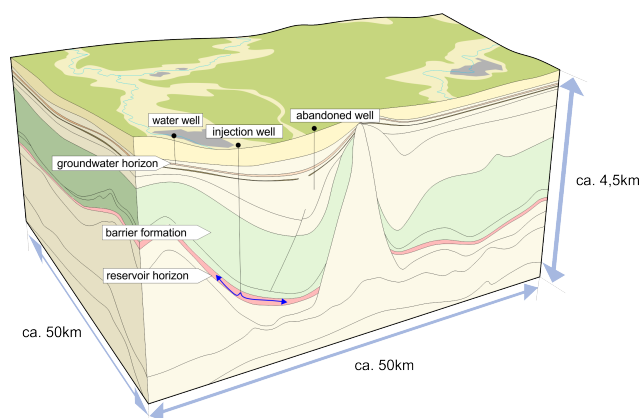


**Figure 3.** Sketch of the geological model used for the guideline-based interviews (graphical realization: Jens Rätz).

the flank of a salt diapir/salt wall. This fault zone continues along the whole flank of the salt diapir. Based on this geological model, simulations were carried out as a basis for the discussion at the workshop. These first simulations included, among others, a permeable fault zone and the injection of water instead of CO<sub>2</sub>. The transport of salt was not included at that stage.

## 2.2 Stakeholder interviews

5 Ten face-to-face interviews were conducted by the social scientists with interviewees representing public authorities, business and industry, the science community, and independent experts. Key issues addressed referred to parameters and processes influencing brine migration, and the specification and prioritization of brine migration scenarios. The social scientists provided interviewees with some detailed questions jointly compiled with the geo-modelers along with the previously introduced model sketch shown in Fig. 3 in order to get the stakeholders' critical feedback on their understanding of brine-related risks and the principal geological model setup. A first result from the interviews relates to the conceptualization of 'damage' in case brine would come into contact with drinking water. Some stakeholders favored an absolute understanding, talking of damage as soon as any salt water intrudes drinking water aquifers. Others hold the opinion that the salinization of groundwater needs to be considered in relative terms. For the latter experts, damage is not a question of whether or not brine gets in contact with groundwater, but is rather defined as an event where specific threshold values are exceeded. This means, in order to allow judgments on risks, a detailed assessment of the brine quantity and its salinity needs to be performed. This issue remained largely unsolved during the interviews and hints to differing concepts, perceptions or interests that may frame the interviewees' risk-related thinking.

As to potential brine migration paths, the interviewed stakeholders unanimously made a clear-cut distinction between man-made and geology induced risks. The former comprises facilities such as old and new boreholes or drinking water wells while geology induced risks refer to cracks and faults, salt diapirism/doming, thin and non-continuous seal or non-continuous Rupelian clay barrier. The distinction between potential migration paths caused by technical installations as well as by geological



**Table 1.** Key elements for scenario building from the interviews.

Element	Stakeholder suggestions
Variable boundary conditions	Consider different boundary conditions since this has considerable impact on brine displacement and pressure increase mechanisms
Variable geology	Use different geological structures since brine displacement and pressure increase is highly dependent on the geological structure
Variable space dimensions	Investigate scenarios with different spatial dimensions (e.g. a large-scale scenario with 100 km)
Man-made migration paths	Integrate drill holes in order to validate expected impacts such as low displacement quantities and minor increase in pressure
Variable parameter values	Use heterogeneous poro/permeability values (rocks) and pressure/density values (fluids)
Injection strategy	Consider different injection points and volumes
Pressure management	Simulate different volumes of brine production
Variable discretization	Work with detailed discretisation of geological weak points vs. rough discretisation of huge spatial structures

structures was accompanied by a distinct risk prioritisation. All participants agreed in estimating geology-based risks as far more relevant compared to man-made risks. In general, interviewees argued that man-made risks, such as a faulty drill hole, are much more easy to cope with technologically and allow only relatively small quantities of brine to migrate.

In addition, a broad range of key elements for scenario building was elicited from the interviews. Table 1 depicts these elements together with stakeholders' suggestions how to integrate them into brine migration scenario modeling.

Several stakeholder suggestions on the geological model, possible scenarios and the relevant physical processes were fed back to the geo-modelers. In order to get feedback on both the setup of the geological model and numerical simulation scenarios, preliminary simulation results were presented at the stakeholder workshop.

### 2.3 Stakeholder workshop

A total of 21 participants attended the workshop representing public authorities, business and industries, and the science communities in the fields of geosciences. Within the first session, geo-modelers presented both the geological model as well as the preliminary simulation results. During the second part of the workshop, a world café deliberation was carried out. For that purpose, the participants were divided into several small groups seated around tables discussing predefined core questions.



After 20 minutes, the groups were recombined in the way that each member of a group moved to a different table. Only one person, the host, remained at the table and informed the new group about what had happened in the previous discussions. This procedure was reconvened three times while discussions focused on the following two sets of questions:

- Set of questions 1) Basic assumptions of the geological model are the spatial dimension of 58 x 39 km and a permeable fault zone along the salt wall. How do you evaluate these assumptions? Is the spatial dimension sufficient to investigate pressure effects in the far-field of the CO<sub>2</sub> injection?

Stakeholder comments differed depending on whether one or multiple injection points are considered. In case of injecting CO<sub>2</sub> at various sites participants unanimously agreed that due to pressure interference a wider space must be investigated. Contrasting opinions had been raised for modeling just a single injection point. One group said the assumed space size of 58 x 39 kilometer is sufficient. The reason for this view relates to the fact that the brine primarily follows vertical migration pathways. Other participants challenged this argument by referring to studies that demonstrate a rise in pressure even in distances of 100 and more kilometers. Hence, according to this, researchers must use models with spatial parameters of this scale in order to create reliable scenario findings.

- Is brine migrating along a salt wall up to the top of the salt diapir realistic?
- The discussion of this question resulted in contrary opinions affirming and denying it. For some stakeholders the existence of permeable pathways along flanks of salt diapirs is basically conceivable. Others are convinced that this is not a realistic assumption and thus found it implausible to model leakage at the salt diapir. Salt would not dissolve at the wall since water in contact with it would already be saturated. The different views to brine migration at salt diapirs finally led to the recommendation to simulate comparative scenarios with high and low permeability parameters for the fault zone along the salt wall. This demand was already in agreement with the modeling approach.

- Set of questions 2) We consider a realistic, but not site-specific model. Is this, in your opinion, an appropriate approach for gaining general insights into brine migration with scenario modeling?

The majority of the stakeholders endorsed the modeling approach by confirming that generic findings could be drawn from a realistic but not site-specific model. Key aspects in terms of processes, methods and structures are covered allowing the model to be used for improving the understanding of some fundamental problems already before an exploration drilling takes place. Of course, stakeholders were aware that working with a realistic model could not substitute a site-specific exploration. This insight was the starting point for a minority of participants to stress that given the issues at stake only geological on-site investigations would be able to deliver reliable findings.

The final session of the workshop consisted of a plenum discussion of the findings from the world café conversations. Here stakeholders made the following additional comments on the preliminary simulation results:

- The injection of brine into a brine-filled storage horizon instead of CO<sub>2</sub> was considered a valid assumption
- The assessment of dynamic effects in the groundwater system during the injection of CO<sub>2</sub> has been seen as a valuable contribution for understanding pressure conditions and fluid migration processes in complex geological systems.





- The stakeholders found it useful to identify the zones where highest local flow rates occur, if the effect of fluid and rock compressibility on the storage capacity of the system is exhausted
- The simulations should include the variable-density flow of brine in future
- Groundwater recharge as a boundary condition for the top aquifers (target aquifers) should be considered

## 5 2.4 Feedback to modeling

From the viewpoint of the geo-modelers, there were three major categories of dealing with stakeholder recommendations resulting from the interviews and the workshop: (i) Those recommendations that coincide with what was already planned; (ii) those recommendations that were not planned but are realized now; and (iii) the recommendations that were not realized, either because they were beyond the scope of the project or deemed less relevant than others by the geo-modelers. Categorized into

10 (i) are the variable-density transport of dissolved salt and the variable parametrization (permeability) of the fault zone along the salt wall. Within category (ii) the implementation of groundwater recharge for the top aquifers to establish more realistic flow conditions is considered. Another point in this category is the lateral extension of the model domain up to 100 km to obtain more realistic lateral boundary conditions similar to an infinite aquifer. The recommendations not considered (category iii) were

15 man-made risks, such as leaky wells, as these were considered much less important than geological risks by the stakeholders. Variable injection volumes/rates were not considered as brine migration rates could be inter- or extrapolated (superposition) from the results presented later. Further pressure management certainly is an interesting topic but could not be addressed within this work. The same holds for overlapping pressures from multiple injection sites. This would require a basin scale model of the North German Basin which is not available yet.

## 3 Geological model

20 In this section the revised geological model (after the stakeholder workshop) is presented. It is the basis for the numerical model presented thereafter.

The database from the south-western German North Sea provided depth lines of stratigraphical surfaces to construct only the main geological units of the NGB in the 3D structural model. Hence, the stratigraphic succession of the NGB is represented in a simplified fashion in this study. The following eight sets of depth lines of stratigraphical surfaces were available to construct

25 the layers for the 3D structural model: base and top of Zechstein (Permian), base of Middle Buntsandstein (Triassic), base of Upper Buntsandstein (Triassic), top of the Buntsandstein (Triassic), base of Upper Paleocene (Tertiary), base of Oligocene (Tertiary) and base of Quaternary. By means of these data 2D grid surfaces for the respective geological units of the model layers were interpolated using the convergent interpolation technique (software Petrel 2012.1).

The depth position of the base of the Zechstein varies slightly between 3300 m and 4000 m across the model. In contrast,

30 the top of the Zechstein shows a highly differentiated structural pattern due to the mobilization of the Zechstein salt with depth between 3800 m and 350 m. The mobilization of the Zechstein salt affected also the geometry of the overburden. As a

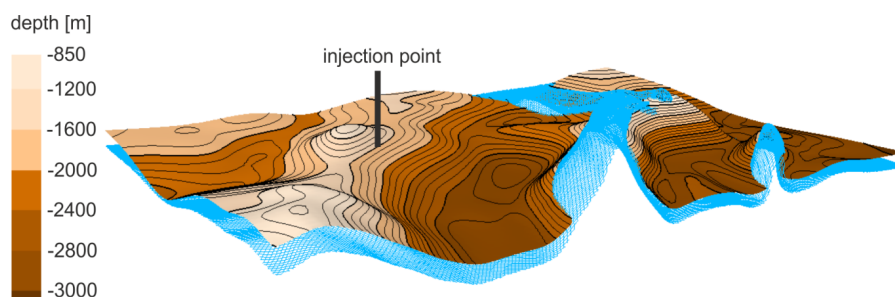


**Figure 4.** Injection point at the flank of the anticlinal structure in about 1600 m depth projected on top of the Solling storage horizon. The top of the Zechstein salt is displayed as blue mesh. Vertical exaggeration is 2:1.

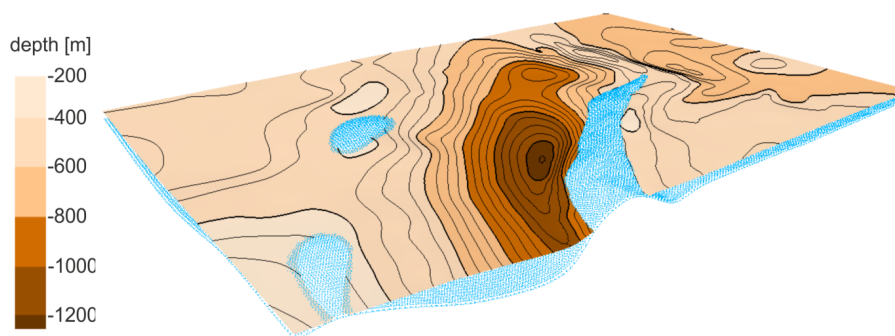


**Figure 5.** Top of the Rupelian clay barrier with discontinuities where Cretaceous sediments penetrate the Rupelian clay barrier. The top of the Cretaceous is displayed as blue mesh. Vertical exaggeration is 2:1.

consequence of this Mesozoic and Cenozoic deposits on top of both the dome structure and the salt wall are uplifted and partly eroded. In order to reflect geological and hydrogeological conditions of a storage complex consisting of a storage horizon and rock barrier systems we added virtual surfaces for important geological units to the final model. The Mesozoic sediments above the mobilized Permian Zechstein salt include the storage horizon and the barrier rocks. The Cenozoic sediments include the

5 Rupelian clay barrier and the fresh water complex. Modifications of the model concerns the layers for the Middle Buntsandstein in which we added two surfaces representing top and base of the Solling sandstone, which acts as the injection horizon for CO<sub>2</sub> (Fig. 4). The overlying geological layer represent rock units of Upper Buntsandstein which act as seal. Furthermore, the top of Oligocene is deemed to be the base of the hydraulically important Rupelian clay barrier in the model to which we added a top surface. We modified this hydraulic barrier to be penetrated by the uplifted Cretaceous sediments on top of the salt

10 dome. Such discontinuities (so-called hydrogeological windows) are also present on top of the rising salt wall where the diapir and overlying Cretaceous sediments pierce into the Rupelian (Fig. 5). Also the layer of both the Tertiary post-Rupelian and the Quaternary are locally pierced by the lifted sediments. To establish more realistic groundwater transport conditions in the shallow aquifer we assigned two Quaternary layers with different hydrogeological properties. As top of the geological model

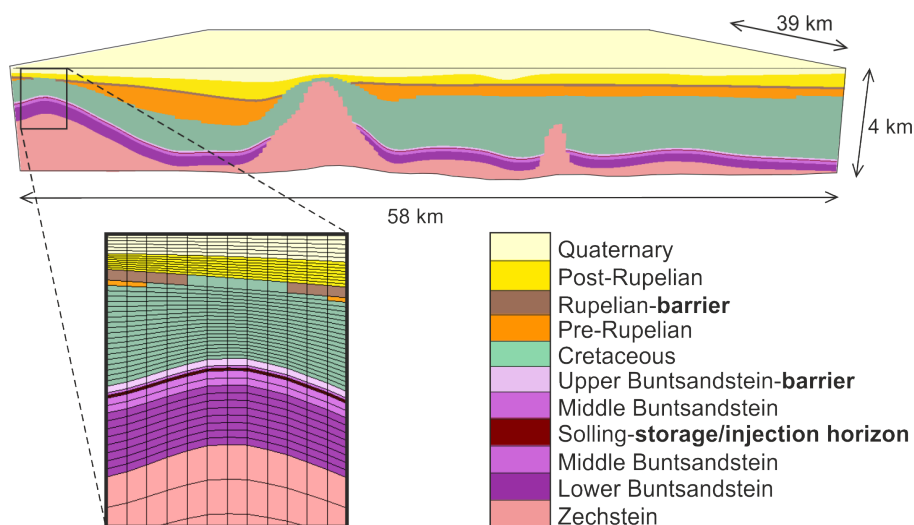


**Figure 6.** Perspective view on the 3D geological model with zoom in on the anticlinal structure showing the mesh of the 3D volume model. Vertical exaggeration 2:1.

we used a dataset of groundwater isolines from an upper freshwater aquifer. In order to simulate the groundwater flow in the shallow Cenozoic aquifers we also used data of main rivers derived from the associated catchment area. Both datasets were prepared to be used as upper boundary condition on top of the model (data provided by LUGV (2012); LUGV (2014)).

Subsequently, the twelve modified 2D grids confining the eleven geological layers of the geological model were merged into a consistent 3D structural model. In the structural gridding process we assigned a consistent cell size of 300 x 300 m horizontally to the 3D cube mesh (Fig. 6).

The vertical resolution depends on the thickness of each layer resolved in the model. In order to sufficiently reproduce the complex geometry we subdivided all layers of large thicknesses resulting in a vertical resolution of less than 300 m for most cells. Each layer is assumed to be homogeneous, i.e. having a single permeability and porosity value assigned to it. Data for lithological composition and the corresponding parameters are derived from regional literature data and numerical simulation studies (Larue, 2010; Reutter, 2011; Schäfer et al., 2011; Noack et al., 2013). Table 2 shows the main lithological compositions, the average thicknesses of the layers, porosity and permeability data assigned to the model layers. Since the Zechstein layer is impermeable it is not included in the simulations, except for the salt wall. As can be seen in the table the Quaternary is split into two parts. With the top part having an increased permeability resulting from a stationary calibration which was performed to obtain a reasonable pressure distribution in agreement with the groundwater isolines and the recharge boundary conditions applied at the top. Further, fault zone permeability and porosity of the reference setting are shown in the table.



**Table 2.** Properties of the model layers according to Larue (2010); Reutter (2011); Schäfer et al. (2011); Noack et al. (2013).

Layer	Lithology	Thickness [m]	Porosity [%]	Permeability [m <sup>2</sup> ]
Quaternary 1	sand, gravel	100	20	$6 \cdot 10^{-11}$
Quaternary 2	sand, gravel	200	20	$1 \cdot 10^{-12}$
(Tertiary) Post-Rupelian	sand, silt	400	15	$1 \cdot 10^{-13}$
(Tertiary) Rupelian	clay	80	10	$1 \cdot 10^{-18}$
(Tertiary) Pre-Rupelian	sand, sandstone	350	10	$1 \cdot 10^{-13}$
Cretaceous	chalk, claystone	900	7	$1 \cdot 10^{-14}$
Upper Buntsandstein	salt, anhydrite, claystone	50	4	$1 \cdot 10^{-18}$
Upper Middle Buntsandstein	siltstone	20	4	$1 \cdot 10^{-16}$
Solling	sandstone	20	20	$1.1 \cdot 10^{-13}$
Lower Middle Buntsandstein	siltstone	110	4	$1 \cdot 10^{-16}$
Lower Buntsandstein	clay- and siltstone	350	4	$1 \cdot 10^{-16}$
Permian Zechstein	rock salt	-	0.1	$1 \cdot 10^{-20}$
Fault zone	-	50	30	$1 \cdot 10^{-12}$

## 4 Numerical model

Models with different conceptual complexity regarding the implemented physics are used in this work, all of them implemented into the open-source numerical simulator DuMu<sup>x</sup> (Flemisch et al., 2011; Schwenck et al., 2015). DuMu<sup>x</sup> was used for a number of problems in the field of CO<sub>2</sub> storage in geological formations (Walter et al., 2012, 2013) and was part of several code comparison studies (Nordbotten et al., 2012; Class et al., 2009).

### 4.1 Model types

Three model types are compared in this work which differ with respect to components and phases considered. The reference model is a single phase (brine), two component (water and salt) model from now on referred to as 1p2c model which accounts for variable-density flow. Simplifying this model by neglecting salt transport leads to a single phase, one component model referred to as 1p1c, where salt is considered as a pseudo component which influences the brine viscosity and the density (similar to a constant geothermal gradient) but the salinity stays constant during the simulation. The third model accounts for two-phase flow (brine and CO<sub>2</sub>) as well as three component (water, CO<sub>2</sub> and salt) transport and is referred to as 2p3c model. In all models the compressibility of the porous medium and the fluid phases is considered. The equations of state used in the models are given in Table 3. Energy transport is not considered but a constant geothermal gradient of 0.03 K/m is applied. The balance equations along with more detailed explanations are given in the Appendix A.



**Table 3.** List of equations of state used for calculating the fluid properties of CO<sub>2</sub> and brine as well as relationships for capillary pressure and relative permeability. The salinity is defined as kg NaCl per kg brine.

	Symbol	Unit	Function of ...	Reference
Density CO <sub>2</sub>	$\rho_n$	$kg/m^3$	$f(p, T)$	Span and Wagner (1996)
Dynamic viscosity CO <sub>2</sub>	$\mu_n$	$Pa \cdot s$	$f(p, T)$	Fenghour et al. (1998)
Density brine	$\rho_w$	$kg/m^3$	$f(p, T, \text{salinity})$	Batzle and Wang (1992) Adams and Bachu (2002)
Dynamic viscosity brine	$\mu_w$	$Pa \cdot s$	$f(T, \text{salinity})$	Batzle and Wang (1992) Adams and Bachu (2002)
Capillary pressure	$p_c$	$Pa$	$f(S_n)$	neglected
Relative permeability	$k_r$	-	$f(S_n)$	Brooks and Corey (1964)

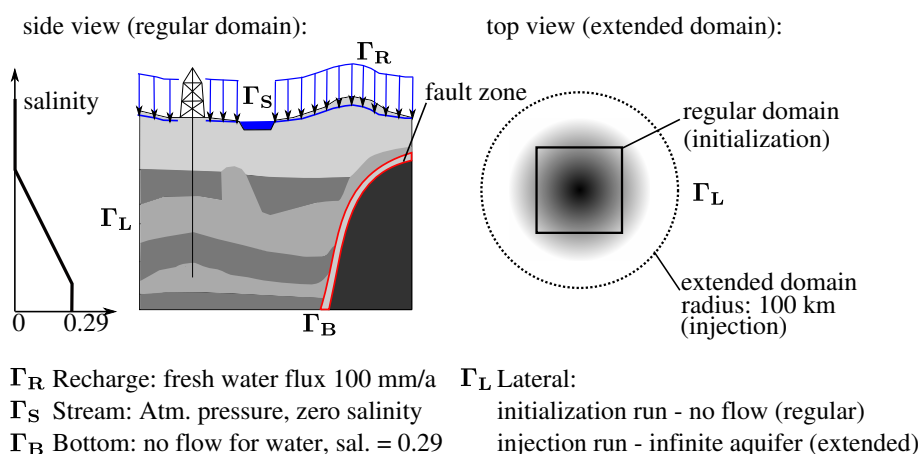


**Figure 7.** Boundary and initial conditions of the domain. A linear salinity profile increasing with depth up to a maximum salinity (salt mass fraction) of  $0.29 \frac{kg-NaCl}{kg-Brine}$  is assumed as an initial condition for the initialization run. Also shown is the position of the fault zone situated on the flank of the salt wall in red.

## 4.2 Initial and boundary conditions

Realistic boundary and initial conditions are required to predict the movement of the displaced brine. The boundary conditions are shown in Fig. 7. On the top boundary ( $\Gamma_R$ ), a constant recharge is set (Neumann boundary condition) except for the finite volumes close to a river ( $\Gamma_S$ ), where a constant atmospheric pressure is set (Dirichlet boundary condition). The rivers,

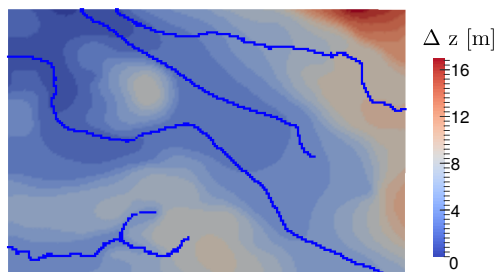


**Figure 8.** Top view on the groundwater table. The rivers are highlighted in blue. The elevation values are normalized to the minimum elevation of the groundwater table.

effectively, act as a sink in the system. Fig. 8 shows the top view of the domain with the elevation of the groundwater table and the rivers. Note that the differences in the elevation of the groundwater table are rather small (17 m). The following assumptions are made:

- All recharge water is drained into rivers within the domain (side boundaries closed).
- 5
- Full hydraulic contact between rivers and groundwater.

During an initialization run, which is required for all models to establish the base flow, the bottom and lateral boundaries are closed for water. However, salt may enter the system for the 2p3c and the 1p2c models at the bottom boundary or the salt wall, where a fixed maximum salinity of  $0.29 \frac{\text{kg-NaCl}}{\text{kg-Brine}}$  is set. The salt wall acts as another source of salt with the fixed maximum salt mass fraction assigned to it. The initialization run for the 1p1c model is straightforward, since the system is almost linear and a steady-state base flow can be established within a single large time step. For the models that consider salt transport (1p2c and 2p3c), an initial salt distribution is prescribed to the system which changes over time according to the boundary conditions. The initialization run is terminated after 300,000 years. On the time scale of the injection and post injection run (100 years) a quasi-stationary system has established by then, i.e. no changes in the concentration field occur. The results from the initialization run serve as the initial condition for the injection runs. During the injection runs, the domain is extended laterally for layers with a permeability greater than  $1 \cdot 10^{-15} \text{ m}^2$  beneath the Rupelian barrier (i.e. Pre-Rupelian, Cretaceous and Solling). The layers are extended to a distance of 100 km from the center of gravity of the regular domain. This distance is sufficient to make the boundaries of the regular domain act as infinite aquifers.

10

15

## 5 Results

This section is sub-divided into three parts. (i) the target variables used in the following parts are briefly discussed, followed by (ii) the results of the scenario analysis and (iii) the comparison of models of different physical complexity. All scenarios and model comparisons are evaluated against a reference model which is by no means the most likely geological setup but is rather

20

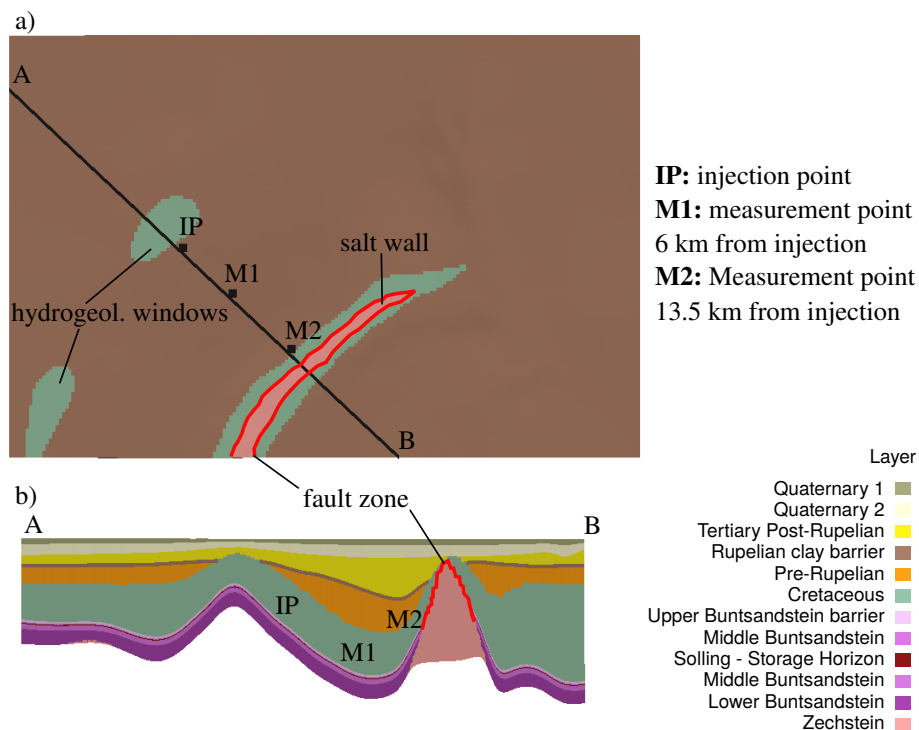


**Figure 9.** a) top view on the Rupelian clay barrier. Also shown are the two hydrogeological windows in the Rupelian clay barrier layer and the salt wall piercing through the barrier layer. The fault zone is highlighted in red. b) shows a cross-section (vertical exaggeration 4:1) across line A-B with approximate locations of the injection point (IP) and the two measurement points for pressure (M1 and M2).

chosen because all processes under investigation occur on a recognizable scale. The setup of the reference scenario is given in Table 4.

### 5.1 Definition of target variables

In order to compare the results different target variables are used:

- 5 – **Flow into target aquifers:** The target aquifers are defined here as everything above the Rupelian clay barrier layer that could potentially be used for drinking water production. Different areas over which the flow (salt flow, brine flow or volume flow) is summed up are distinguished: (i) flow near the salt wall, which comprises the flow through the fault zone and the flow through the Cretaceous dragged up by the salt wall (for ease of notation we refer to both as flow through the fault zone), (ii) flow through the hydrogeological windows in the Rupelian clay barrier and (iii) total flow
- 10 into the target aquifers comprising (i) and (ii) as well as the flow through the intact Rupelian clay barrier. Figure 9 shows a view on the interface between the Rupelian clay barrier layer and the target aquifers. Further, the total salt flow into the more shallow Quaternary 2 is also considered.



**Table 4.** List of parameters for the reference setting. The two phase flow specific parameters are only required for the 2p3c model.

Parameter	Unit	Value
Compressibility solid phase	$\text{Pa}^{-1}$	$4.5 \cdot 10^{-10}$
Depth injection	m	1651
Temperature gradient	$\text{Km}^{-1}$	0.03
Temperature top	K	281.15
Density $\text{CO}_2$ at injection point	$\text{kgm}^{-3}$	687
Density brine at injection point	$\text{kgm}^{-3}$	1078
Injection rate $\text{CO}_2$	$\text{kgs}^{-1}$	15.9 ( $0.5 \frac{\text{MT}}{\text{year}}$ )
Volume-equivalent injection rate brine	$\text{kgs}^{-1}$	24.9
Recharge at top boundary	mm/year	100
Initial salinity gradient	$\text{gL}^{-1}(100\text{m})^{-1}$	15
Maximum salinity	$\frac{\text{kg}-\text{NaCl}}{\text{kg}-\text{Brine}}$	0.29
Two-phase flow specific parameters:		
Brooks and Corey shape parameter $\lambda$	-	2.0
Residual water saturation	-	0.2
Residual $\text{CO}_2$ saturation	-	0.05

- **Pressure rise at selected locations:** Pressure rise due to the injection is monitored during the simulation at two locations (M1 and M2) in the injection horizon Solling, which are on a straight line between the injection point and the nearest point on the salt wall: (i) M1 approximately 6 km from the injection and (ii) M2 approximately 13.5 km from the injection directly on the fault zone on the salt wall, see Fig. 9 b).
- 5 - **Concentration changes in target aquifers:** The injection-induced changes in the salt concentration will be shown on the top of the Rupelian clay barrier as shown in Fig. 9 a) and on the top of the Post-Rupelian.

## 5.2 Scenarios analysis

In this section four different scenarios are evaluated each varying a key parameter (initial salt distribution prior to the injection, lateral boundary conditions, role of the Upper Buntsandstein barrier permeability and the fault zone transmissibility). The setup of the reference scenario is given in Table 4.

### 5.2.1 Scenario 1: Initial salt distribution

As described in the previous section, an initial salt distribution serves as the initial condition of the initialization run which covers 300,000 years. The initial salt distribution is applied as a gradient of increasing salinity with depth, starting at 645 m



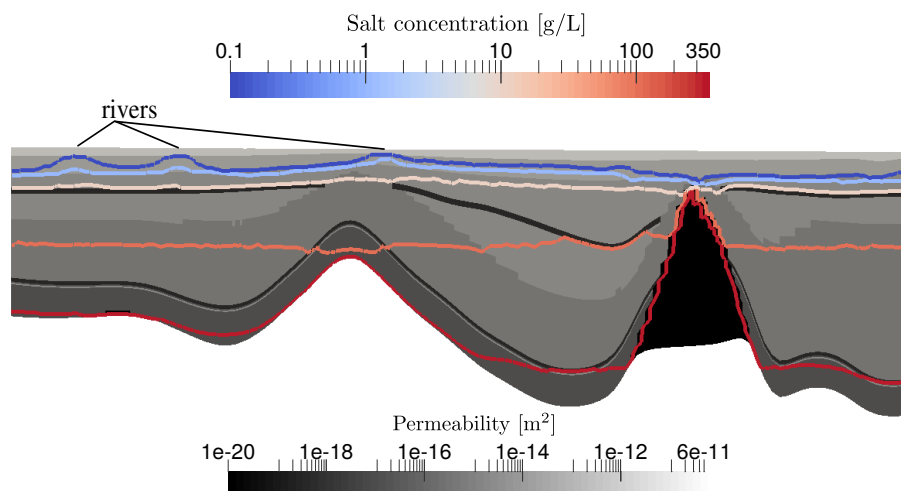


**Figure 10.** Salt distribution for the medium (reference) case after 300,000 years initialization run along the cross-section shown in Fig. 9 (vertical exaggeration 4:1). Six concentration-isolines are shown which correspond to the entries in the legend (0.1, 1, 10, 100 and 300). The permeability of the different layers is also shown. Please note the logarithmic scale of concentration and permeability.

which is the average depth of the Rupelian clay barrier layer. Once the maximum salinity is reached at a certain depth, it does not increase further (see Fig. 7). Three different scenarios with different gradients are considered: low, medium, and high. The gradient is decreased to 10 (low) and increased to  $20 \text{ gL}^{-1}(100\text{m})^{-1}$  (high) from the reference value of  $15 \text{ gL}^{-1}(100\text{m})^{-1}$  (medium). First we look at the state of the system in Fig. 10 after the initialization run when a quasi-stationary system has established for the medium case (reference case). The salt distribution has considerably changed from the initial salt gradient (not shown here). The less dense brine has migrated above the Rupelian clay barrier while the more dense brine collects at the bottom of the domain. The salt distribution changes the most during the first 50,000 years. The initialization run shows that upconing in the target aquifers occurs near rivers. The rivers represent sinks since the lowest potential in the system (atmospheric pressure, zero salinity) is assigned there. The 10 g/L isoline closely follows the Rupelian clay barrier layer except where the depth of the Rupelian clay barrier layer strongly increases near the salt wall. The concentration changes after 50 years of injection (i.e. the end of the injection) are shown in Fig. 11. While concentration changes of up to 3 g/L occur at the top of the Rupelian clay barrier, maximum concentration changes on the top of the Tertiary Post-Rupelian directly below the Quaternary are an order of magnitude smaller 0.25 g/L. The largest changes occur close to the fault zone and via the hydrogeological window above the injection horizon. Generally, the concentration changes due to the injection increase from the low to the high scenario as the salt concentrations obtained from the initialization run are higher and, therefore, more salt can be displaced by the injection. This is illustrated in Fig. 12. Here, the total salt flow across the Rupelian clay barrier (left) and the Tertiary Post-Rupelian (right) are plotted over the injection and post-injection period. While the base flow of salt is almost the same for the two layers, the rise due to the injection is much more pronounced at the top of the Rupelian clay barrier where the initial concentration is higher, especially near the salt wall. Therefore, the magnitude of concentration increase after

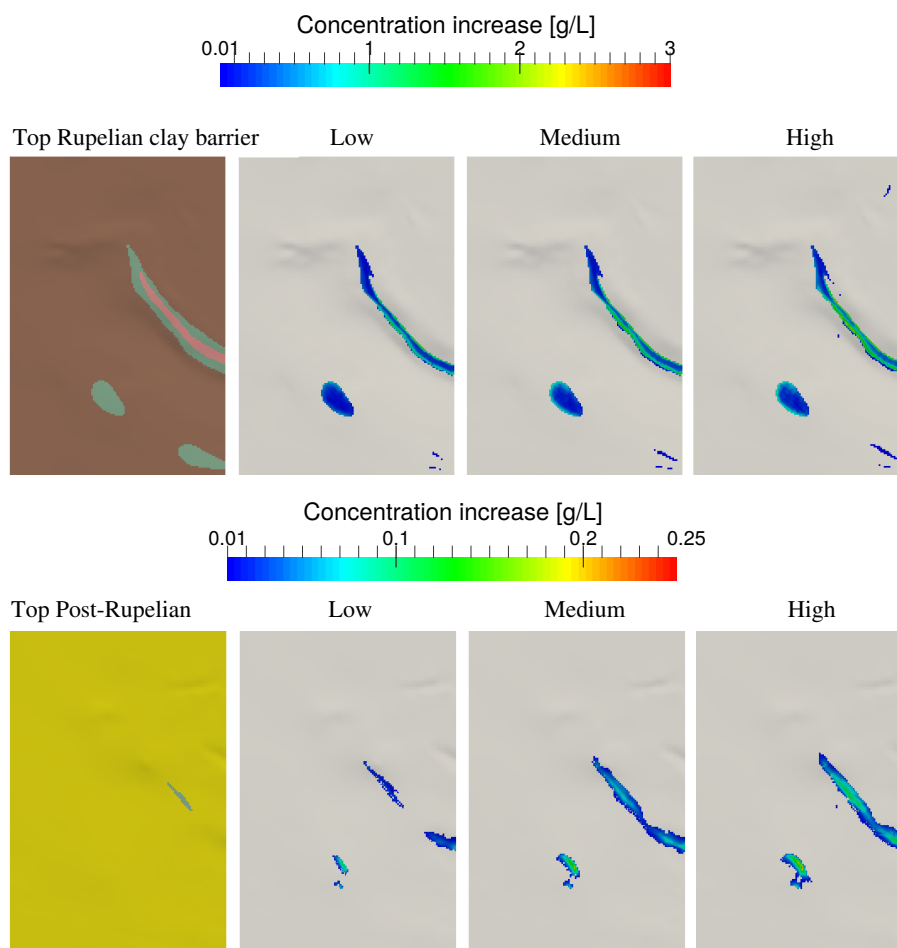


**Figure 11. Top row:** view on top of the Rupelian clay barrier for three different scenarios low, medium and high with increasing initial salt gradients. The results show the salt concentration increase after 50 years of injection. Concentration increases below 0.01 g/L are not shown. **Bottom row:** view on top of the Post-Rupelian for the three cases, see Fig. 9 b) for orientation. Note the different scales on the legends for the top and bottom row.

the injection mainly depends on the initial salt distribution used for the injection run or in other words a notable increase in concentration will probably only occur where elevated salt concentrations already exist prior to the injection.

### 5.2.2 Scenario 2: Boundary conditions

In this scenario, three different boundary conditions for the lateral boundaries of the regular domain are compared. The reference case uses a domain extension which results in an infinite aquifer behavior as already described above. The other two cases use a no-flow and a Dirichlet boundary condition (hydrostatic) respectively on the lateral boundary of the regular domain. The results are shown in Fig. 13 for the three cases. It can be seen that the choice of boundary conditions strongly influences

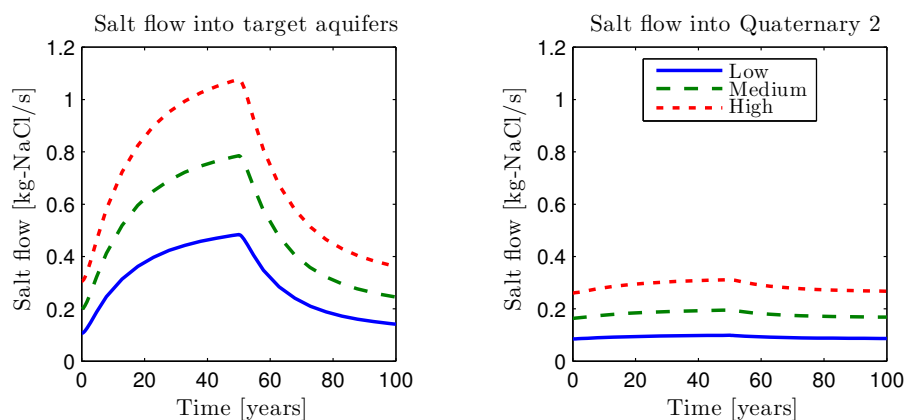


**Figure 12.** **Left:** salt mass flow over the top of the Rupelian clay barrier into the target aquifers. **Right:** salt mass flow over the Tertiary Post-Rupelian into the Quaternary 2.

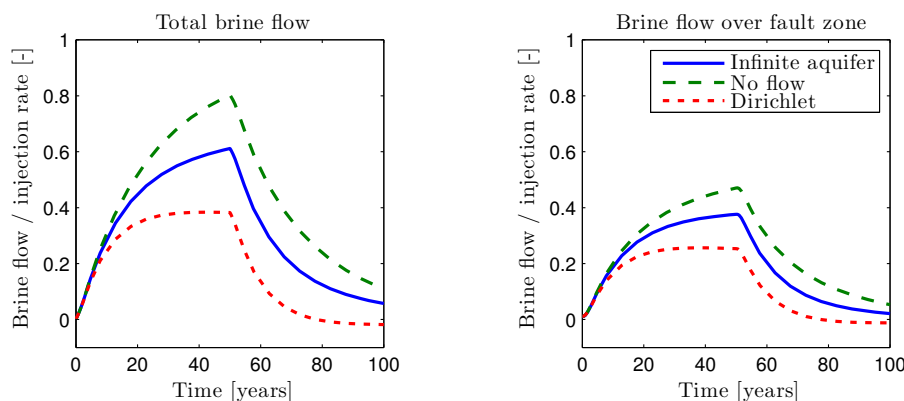


**Figure 13.** **Left:** total brine flow into the target aquifers normalized by the injection rate. **Right:** brine flow over fault zone into the target aquifers.

the overall flow regime in the whole system. For the no flow case considerably more fluid is displaced vertically than for the Dirichlet case. The infinite aquifer case is somewhere in the middle of the other two cases which is expected since more storage capacity is available in the extended aquifers than for the no flow case and a stronger resistance to flow at the lateral boundaries is established than in the Dirichlet case. For the infinite aquifer case the total flow into the target aquifers reaches a level of about 60% of the injection rate. The rest is stored within the compressible brine and rock phases.

### 5.2.3 Scenario 3: Upper Buntsandstein barrier permeability

Within this scenario, the permeability of the layer confining the injection layer i.e. Upper Buntsandstein barrier is varied over several orders of magnitude. The results are presented in Fig. 14. The higher the Upper Buntsandstein barrier permeability the

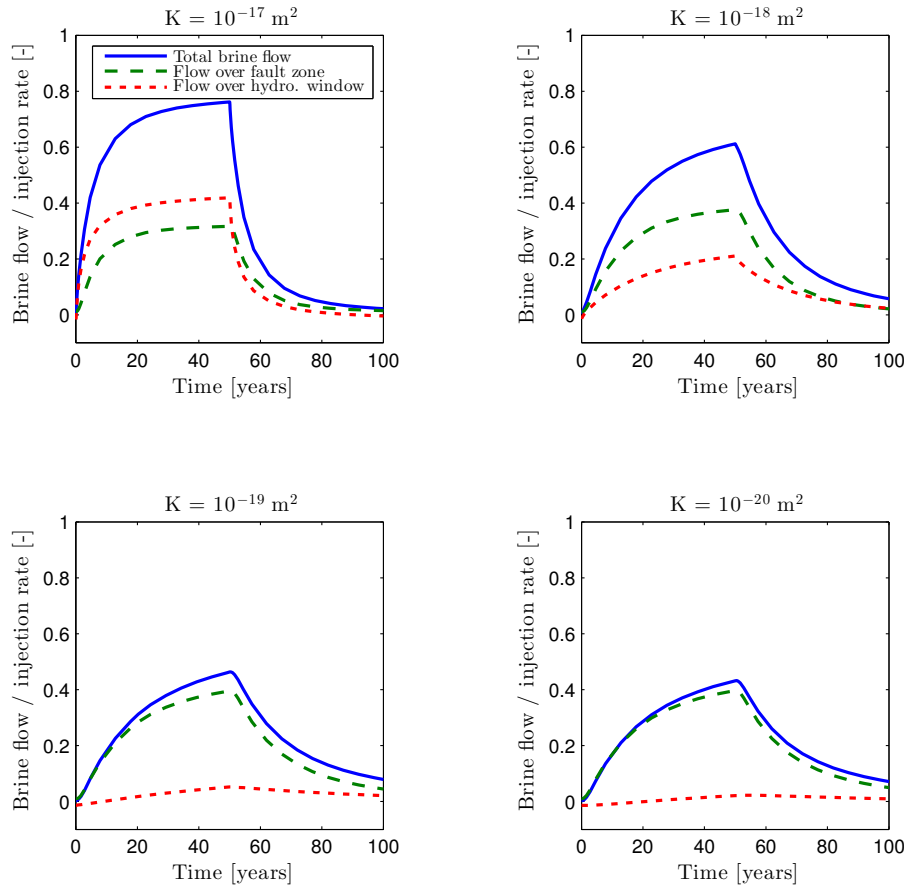


**Figure 14.** Brine flow normalized by the brine injection rate into the target aquifers, for different permeabilities of the Upper Buntsandstein barrier. The upper right scenario with a permeability of  $1 \cdot 10^{-18} \text{ m}^2$  corresponds to the reference scenario.

more diffuse leakage through this barrier will occur resulting also in increased flow through the hydrogeological window in the Rupelian clay barrier directly above the injection. The flow field completely changes when decreasing the barrier permeability and focused leakage through the fault zone becomes the predominant leakage path. The overall amount of displaced fluid into the target aquifers decreases with decreasing barrier permeability. Diffuse leakage becomes less important at low barrier rock permeabilities between  $1 \cdot 10^{-19}$  and  $1 \cdot 10^{-20} \text{ m}^2$ . The simulations show the importance of the Upper Buntsandstein barrier permeability in controlling diffuse leakage through the barrier and focused leakage through the fault zone.

#### 5.2.4 Scenario 4: Fault zone transmissibility

In this scenario, the fault zone transmissibility is varied by changing its permeability for two cases: (i) case with high diffuse migration where the permeability of the barrier rock is similar to the reference case ( $1 \cdot 10^{-18} \text{ m}^2$ ) and (ii) case where the permeability of the barrier rock is low ( $1 \cdot 10^{-20} \text{ m}^2$ ) and migration mainly occurs through the fault zone. The results are

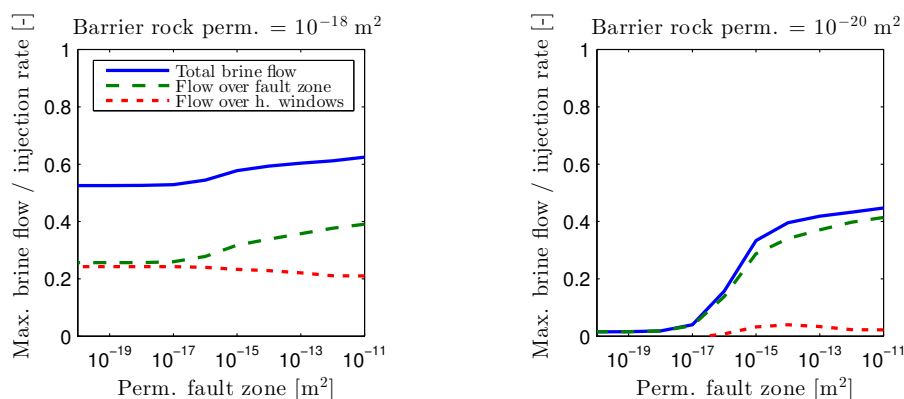


**Figure 15.** Maximum brine flow into the target aquifers reached after 50 years of injection normalized by the injection rate over the fault zone permeability, for two different permeabilities of the Upper Buntsandstein barrier. **Left:** high barrier permeability, high diffuse migration over barrier; **right:** low barrier permeability, high focused migration over fault zone.

presented in Fig. 15. While varying the fault zone permeability also has a notable effect where diffuse migration is dominant (left figure), the effect is considerably higher for the case with focused migration (right figure), especially for fault zone permeabilities between  $1 \cdot 10^{-17}$  and  $1 \cdot 10^{-14} \text{ m}^2$ . For higher permeabilities of the fault zone the flow is less sensitive to changes in the permeability as the resistance of the fault zone becomes small compared to the resistance within the injection layer. The right figure also shows that if neither a diffuse nor focused vertical pathway up to the target aquifers exists, vertical migration does not occur.

### 5.3 Model simplification

The results of three different model comparisons are shown in this section. All comparisons are carried out against the reference setup for the 1p2c model given in Table 4. As target variable the volumetric flow into the target aquifers is chosen as this indicates how well the flow fields match.

#### 5.3.1 Comparison 1: Neglecting salt transport

In this comparison, we discuss the effect of neglecting salt transport and the effects of variable-density flow by comparing the 1p2c model with the 1p1c model. For the 1p1c model the salinity is set as a pseudo component (similar to temperature) influencing the brine density and viscosity but with a fixed value throughout the simulation. A constant salinity increasing with depth at a rate of  $15 \text{ g/L}/100\text{m}$  is assigned similar to the condition assigned to the 1p2c model before the initialization run. The 1p1c model does not require any initialization and the results are therefore much faster to obtain. Brine is injected at a rate of  $25.2 \text{ kg/s}$  in the 1p1c model which is the volume-equivalent rate corresponding to the  $24.9 \text{ kg/s}$  injected in the 1p2c model due to different densities at the injection point (1p1c:  $1091 \text{ kg/m}^3$ ; 1p2c  $1078 \text{ kg/m}^3$ ). The results for the volumetric flow into the target aquifer are shown in Fig. 16. The total volumetric flow of the 1p1c model is higher by approximately 3.5% at the end

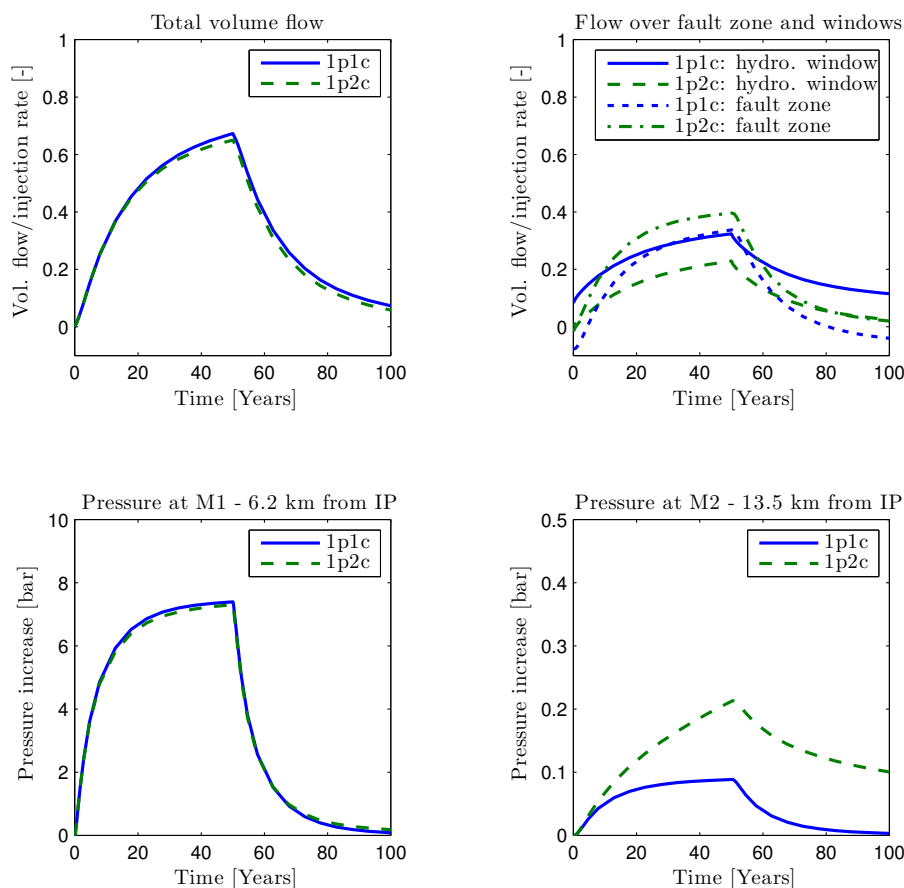


**Figure 16. Top row:** volumetric flow normalized by the volumetric injection rate over time into the target aquifers for the 1p1c and the 1p2c model. **Bottom row:** pressure increase due to injection at M1 and M2.

of the injection. The volumetric flow over the fault zone and the hydrogeological windows for the 1p1c model (see top right of Fig. 16) starts at a value below (fault zone) and above (hydrogeological window) zero, which is due to the base flow induced by the recharge boundary conditions on the top boundary. For the 1p1c model, the water entering the layers below the Rupelian clay barrier over the fault zone leaves again over hydrogeological windows with the total net flow being zero. Hence, the total volumetric flow into the target aquifers before the injection is also at zero. For the 1p2c model, the overall exchange of water between the target aquifers and the layers below the Rupelian clay barrier is much smaller than for the 1p1c, as the salt water needs to be moved against the gravitational forces. For the 1p1c model the baseflow and the injection induced flow have the same order of magnitude whereas for the 1p2c the injection induced flow is much larger than the base flow. On the bottom row of Fig. 16 the pressure increase at M1 and M2 are shown (see Fig. 9 for the approximate location). The pressure increase 6 km from the injection (M1) is almost the same for both models as the brine viscosity in the injection layer is similar. However, at the fault zone the pressure increase for the 1p2c is higher by a factor of approximately two compared with the 1p1c model

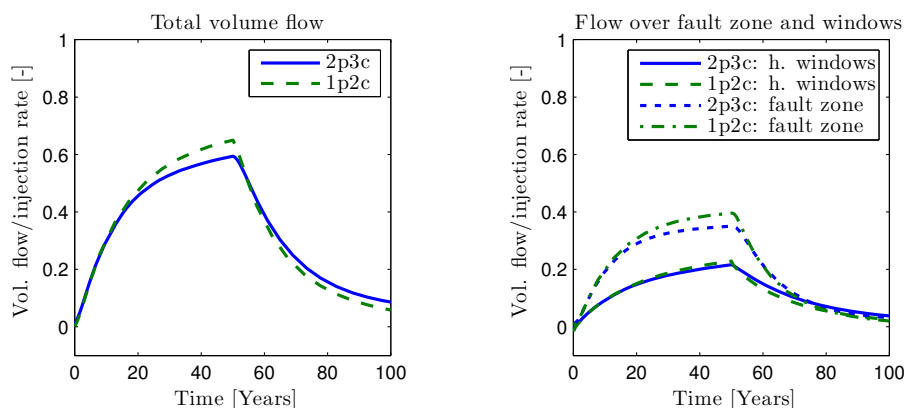


**Figure 17.** Volumetric flow normalized by the volumetric injection rate over time into the target aquifers for the 2p3c and the 1p2c model.

which is due to the increasing weight of the brine within the fault zone leading to an increasing resistance. This is a result of variable-density salt transport.

### 5.3.2 Comparison 2: CO<sub>2</sub> versus water injection

Now the 1p2c and the 2p3c model (where CO<sub>2</sub> instead of brine is injected) are compared. As the injection point is located on the flank of the anticline, buoyancy forces drive the CO<sub>2</sub> upwards (see Fig. 9 for the approximate position of the injection point). The results are shown in Fig. 17. The total volumetric flow for the 1p2c model is higher by 9.5% compared with the 2p3c model. The rise in pressure near the injection causes the density of CO<sub>2</sub> to increase which leads to a reduced brine flow into the target aquifers. For the 1p2c, where a volume-equivalent brine injection rate is used based on the initial conditions at the injection point, this effect is negligible due to the very small compressibility of brine. Additionally, the upward movement of the CO<sub>2</sub> plume along the anticline leads to a reduction of the brine flow into the fault zone as the CO<sub>2</sub> plume moves away from the fault zone.

### 5.3.3 Comparison 3: Simplifying the geometry

The last comparison deals with a major simplification of the geometry. The reference case here is called "complex" while the simplified geometry is referred to as "generic". The generic model considers variable-density salt transport. In the generic case the complex geometry is converted into a simple stratified system with the layering orthogonal to the direction of gravity as shown in Fig. 18. The target aquifers are removed and replaced by a Dirichlet boundary condition with a constant hydrostatic pressure and zero salinity above the Rupelian clay barrier. Therefore no baseflow establishes as hydrostatic conditions are assumed within the domain along with a linear salinity gradient similar to the one prescribed initially for the complex case (15 gL<sup>-1</sup>(100m)<sup>-1</sup>). The salt wall is implemented at the boundary of the model domain along with the fault zone marked in red in Fig. 18. The lateral boundary conditions are like in the complex model infinite aquifers. The relevant properties: layer

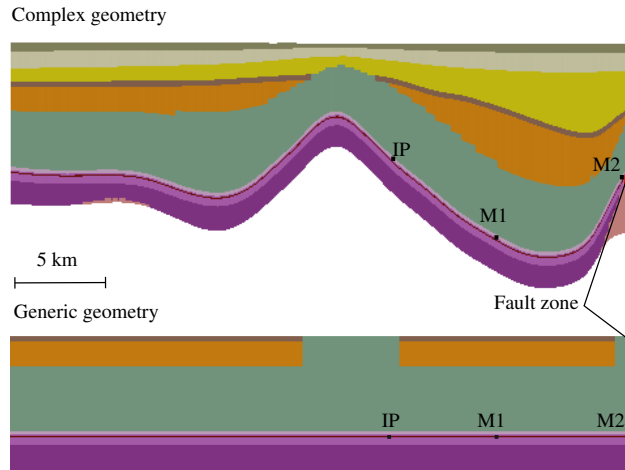


**Figure 18.** Cross-section of the complex and generic geometry (vertical exaggeration 4:1) along the same cross-section shown in Fig. 9.

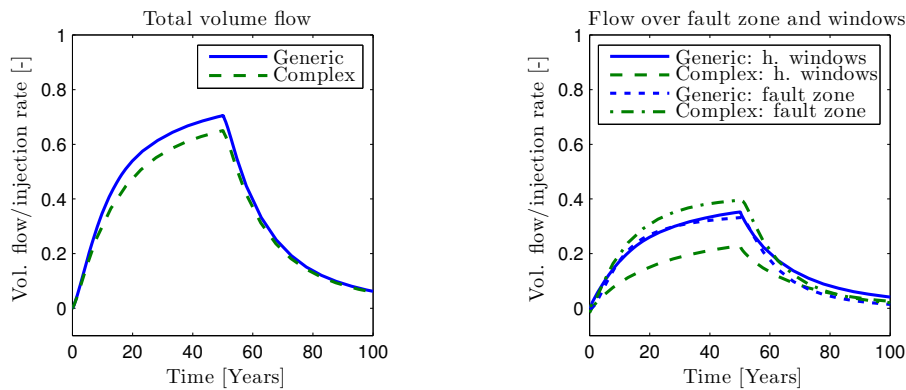


**Figure 19.** Volumetric flow normalized by the volumetric injection rate over time into the target aquifers for the generic and the complex model.

thicknesses, distances of geological features and the areas of the hydrogeological windows are estimated from the complex geometry. Again brine is injected at a rate of 25.8 kg/s in the generic model which is the volume-equivalent rate corresponding to the 24.9 kg/s injected in the complex model due to different densities at the injection point (generic: 1117 kg/m<sup>3</sup>; complex 1078 kg/m<sup>3</sup>). The results are given in Fig. 19. The total volume flow across the top boundary (equivalent to the flow into the target aquifers) for the generic model is 8.5% higher than for the complex model at the end of the injection. The flow across the fault zone and the hydrogeological windows is different with the generic model having higher flow through the hydrogeological windows and less flow through the fault zone. The reason for this difference lies on the one hand in the simplified representation of the geometry of the Cretaceous and the Pre-Rupelian which shifts the path of least resistance but also in the different brine viscosities and densities within the injection horizon for the two models.





## 6 Discussion

Participatory modeling (PM), i.e. involving external experts and stakeholders, has proven to be a helpful and successful approach for brine migration scenarios. Geo-modelers gained valuable feedback and recommendations for their research and knowledge transfer to stakeholders is promoted. The stakeholder workshop received the attention of a more general audience with a newspaper article published in one of Germany's major newspapers [Schrader, 2014]. The groundwork for this positive outcome is the interaction between those three actor groups crucial for the performance of PM processes, i.e. geo-modelers, stakeholders, and social scientists. Openness for stakeholder inputs and the general willingness to adapt models, concepts, or findings in response to stakeholder evaluations are key requirements for geo-modelers in PM processes. This cannot be taken for granted, since the geo-modelers have detailed insights into the problem setting. Hence, in order to be on an equal footing with the geo-modelers, the participating stakeholders must consist of experts, decision-makers, or affected people well-known for their expertise in the respective field. Although stakeholders are experts themselves, they need to comply with predefined framework conditions constraining their influence. The role of the social scientists is twofold. First, they must have comprehensive knowledge about social science methodologies since they need to select the appropriate tools for the specific PM case and they must be experts in applying these methods. Second, the social scientists facilitate the interaction between geo-modelers and stakeholders in terms of both translating research questions into a form which is suitable for stakeholder discussions and stakeholder's feedback, i.e. comments and assessments, to the geo-modelers. Maintaining strict neutrality and concentrating on method and communication expertise are at the heart of the social scientists' facilitator role.

The results presented here are obtained from a revised version of the geological and numerical model after the stakeholder workshop. They show first and foremost that, if we consider concentration changes in the target aquifers as the key variable for estimating damage due to CO<sub>2</sub> injection, we need to have a good knowledge of the salt distribution prior to the injection. As the results (see Fig. 11 and 12) show, two conditions need to be fulfilled in order for notable changes in concentration to occur: (i) the permeability is high enough such that flow occurs (this is true where the Rupelian clay barrier is discontinuous), and (ii) some initial concentration is already present prior to the injection. Notable changes in concentration occur only locally which is in qualitative agreement with findings by Tillner et al. (2013) and Kempka et al. (2013).

Another key aspect is the definition of realistic boundary conditions. Assuming Dirichlet conditions at the lateral boundaries during the injection will lead to an underestimation of the vertical migration of brine. No-flow boundaries within the regular domain or extending the model to obtain infinite aquifer conditions will allow significantly higher vertical brine flow as shown in Fig.13. If the top boundary above the target aquifers was considered a no-flow boundary, brine flow into the target aquifers would be significantly smaller as, for example, in Walter et al. (2012, 2013) or Cihan et al. (2013) where the displaced brine distributes more into the intermediate aquifers below the target aquifers.

Of similar relevance is diffuse migration across the barrier layers (especially the barrier layer sealing the injection layer, here: Upper Buntsandstein barrier). Our results show that, if we increase the permeability of the Upper Buntsandstein barrier, the vertical migration of brine increases as the overall vertical resistance decreases. Significant diffuse migration across the barrier will change the flow regime in the intermediate layers (Cretaceous, Pre-Rupelian) resulting in focused migration where



the Rupelian clay barrier is discontinuous (hydrogeological windows), even if the Upper Buntsandstein barrier below is intact (see Fig. 14). Furthermore, diffuse vertical migration is significant for permeabilities higher than  $1 \cdot 10^{-19} \text{ m}^2$ , which is in good agreement with findings in Birkholzer et al. (2009).

Varying the fault zone transmissibility shows that upward flow is most sensitive to this transmissibility when diffuse migration is small and the resistance from the injection point to the fault zone is in the same range as the resistance within the fault zone. This also means that assuming a simplified geometrical representation of the fault zone will not considerably alter the results compared to a more accurate representation.

Next, the effect of different model assumptions is discussed. In the first comparison, the transport of salt and, thus, variable-density flow is neglected. The corresponding 1p1c model does not require a complex and costly initialization run. Obviously, concentration changes can not be considered as a target variable, but still relevant information on volume flow into the target aquifers can be obtained, which may be a useful target variable for optimizing a pressure management concept. In the 1p1c model, the total volume flow is not significantly higher than in the 1p2c model (see Fig. 16). However, significant differences can be seen in the base flow that establishes below the Rupelian clay barrier which is much higher for the 1p1c model. The 1p1c seems to overestimate the base flow which has the same order of magnitude as the injection-induced flow. When looking at the pressure at the measurement point M1 (6.2 km from the injection) it becomes clear that the overall brine viscosity in the injection layer is met well by setting the salinity as a pseudo component with a linear salt gradient. In M2 (13.5 km from the injection), the pressure increase is about two times as high for the 1p2c model as for the 1p1c model which can be attributed to the increased resistance due to the upward flow of heavy brine. Hence, variable-density flow is important to consider if pressure increase is a target variable.

The second assumption we look at concerns the effect of injecting brine instead of supercritical  $\text{CO}_2$  at a volume-equivalent rate. The total volumetric flow is 9.5% higher for the 1p2c model than for the 2p3c model (see Fig. 17). The injection of brine instead of  $\text{CO}_2$  is therefore a conservative assumption. This assumption has also been previously discussed in the literature for example by Cihan et al. (2013).

The last comparison deals with simplifying the complex geometry of the geological model. A more simple generic system may be advantageous in many cases as the effort of setting up the geological model is reduced and the implementation of geological features is faster, especially if the uncertainty in the location of fault zones were included within a risk assessment approach. However, if the location of the geological features is known, then it is important to have good estimates of the distances and transmissibilities between features since this determines the main flow paths. Additionally, the viscosity differences due to the varying depth of the injection layer in the complex model can lead to a different resistance compared with the generic model. The same arguments hold for analytical solutions which also rely on a simplified geological description. The results show that the total flow into the target aquifers for the generic geometry is overestimated by 8.5% compared with the complex geometry. There are differences with respect to flow across the individual features as can be seen on the right-hand side of Fig. 19. If we are interested in concentration changes as a target variable, the effects of the complex geometry are neglected during the initialization with a generic geometry; hence, a realistic salt distribution can not be obtained. However, the uncertainty related to the simulated salt distribution prior to the injection is quite high and in reality there will probably



not be sufficient data to calibrate the model. Therefore using conservative assumptions as presented in Walter et al. (2012) or Cihan et al. (2013) with a generic geometry can be justified in the light of sparse data availability. Especially the assumption of the salinity distribution near the salt water - fresh water interface will then influence the results of a risk assessment.

## 7 Conclusions

- 5 The main findings of this work are summarized below:
- Involving external experts and stakeholders in geological model building can lead to scenarios for simulating brine migration which are reliably based on a broad agreement. Recommendations resulting from the participatory modeling approach confirmed decisions on scenario design planned earlier on the one hand and, on the other hand, raised issues that were originally not intended for implementation.
  - 10 – Key for a useful PM project is a continuous two-way communication and transfer of knowledge between geo-modelers and external experts facilitated by social scientists who are skilled in deploying the PM method tool box.
  - Stakeholders profit from the knowledge transfer and the possibility to influence the outcome of the PM process.
  - Notable, in the sense of non-negligible, increases in salt concentration in the target aquifers are locally constrained to regions, where initially elevated concentrations are present prior to the injection, and where permeabilities of the Mesozoic strata are high enough to support sufficient flow. Hence, the quality of the prediction of concentration changes  
15 strongly depends on how well the initial salt distribution is known.
  - An inherent problem to modeling is the assignment of boundary conditions. Lateral and top boundary conditions strongly determine the amount of displaced brine into the target aquifers. Lateral Dirichlet boundary conditions at insufficient distance from the injection will lead to a strong underestimation of vertical flow. Setting the top boundary condition as  
20 *open* - as opposed to a closed boundary at the top - strongly increases the amount of fluid that is displaced into the target aquifers.
  - The permeability of the Upper Buntsandstein barrier plays a crucial role in determining the amount of diffuse migration. Diffuse migration over the Upper Buntsandstein barrier can result in focused migration in regions where the Rupelian clay barrier is discontinuous.
  - 25 – During the injection with a constant injection rate, considering salt transport decreases the overall vertical flow due to the additional resistance caused by the increase in the gravitational force. However, the effect of salt transport on vertical flow is not as significant as the pressure increase near the fault zone when salt transport is considered. Hence, if pressure increase is a target variable salt transport should be considered.
  - Injecting an equivalent volume of brine instead of CO<sub>2</sub> is a conservative assumption which leads to higher brine flow  
30 into the target aquifers.



- Simplifying the geometry can lead to comparable results with regard to total vertical brine migration with much less effort required for the setup of the geological model. For real systems, where the uncertainty of the geological model both in parametrization and geometry is high, this implies that a simplified representation of the geometry for the simulations can be considered a feasible and justified approach.

## 5 Data availability

In order to obtain the simulation code DuMu<sup>x</sup> (Version 2.8.0; Schwenck et al. (2015)) has to be installed along with the DuMu<sup>x</sup>-Pub module<sup>1</sup> containing the problem setup and grids. For further information on the installation of DuMu<sup>x</sup> please visit the dumux homepage<sup>2</sup> and look into the README in the DuMu<sup>x</sup>-Pub module.

## Appendix A: Numerical model: Balance equations and solution method

- 10 In this work three model types are compared with each other which differ with respect to the components and phases that are considered. The most complex model is a two-phase three-component model (2p3c):

$$\frac{\partial(\phi \sum_{\alpha} \varrho_{\alpha}^{mol} x_{\alpha}^{\kappa} S_{\alpha})}{\partial t} - \sum_{\alpha} \nabla \cdot \left\{ \varrho_{\alpha}^{mol} x_{\alpha}^{\kappa} \frac{k_{r\alpha}}{\mu_{\alpha}} \mathbf{K}(\mathbf{grad} p_{\alpha} - \varrho_{\alpha} \mathbf{g}) + \varrho_{\alpha}^{mol} \mathbf{D}_{\alpha, pm}^{\kappa} \mathbf{grad} x_{\alpha}^{\kappa} \right\} = q^{\kappa}, \quad (A1)$$

$$\alpha \in \{w, n\} \text{ and } \kappa \in \{H_2O, CO_2, NaCl\},$$

- where the phase index  $\alpha$  represents the phases: wetting (w, brine) and non-wetting (n, CO<sub>2</sub>). The component index  $\kappa$  represents the components water (H<sub>2</sub>O), carbon dioxide (CO<sub>2</sub>) and salt (NaCl).  $\phi$  is the effective porosity,  $\varrho_{\alpha}^{mol}$  is the molar and  $\varrho_{\alpha}$  the mass density of phase  $\alpha$ .  $x_{\alpha}^{\kappa}$  is the molar fraction of component  $\kappa$  in phase  $\alpha$ ,  $S_{\alpha}$  is the saturation,  $k_{r\alpha}$  is the relative permeability,  $\mu_{\alpha}$  is the dynamic viscosity,  $\mathbf{K}$  is the intrinsic permeability tensor,  $p_{\alpha}$  is the phase pressure,  $D_{\alpha, pm}^{\kappa}$  is the effective diffusion coefficient of the porous medium. The model can account for miscibility of the two phases, however we are not primarily interested in the fate of the injected CO<sub>2</sub>, therefore we consider the two phases immiscible. Salt is only present in the brine phase. To conclude the wetting phase consists of the components water and salt and the non-wetting phase only of CO<sub>2</sub>.

Neglecting the effects of two phase flow we arrive at a single-phase, two-component model (1p2c):

$$\frac{\partial(\phi \varrho_w^{mol})}{\partial t} - \nabla \cdot \left\{ \varrho_w^{mol} \frac{\mathbf{K}}{\mu_w} (\mathbf{grad} p_w - \varrho_w \mathbf{g}) \right\} = q_w, \quad (A2)$$

$$\frac{\partial(\phi \varrho_w^{mol} x_w^{NaCl})}{\partial t} - \nabla \cdot \left\{ \varrho_w^{mol} x_w^{NaCl} \frac{\mathbf{K}}{\mu_w} (\mathbf{grad} p_w - \varrho_w \mathbf{g}) + \varrho_w^{mol} \mathbf{D}_{w, pm}^{NaCl} \mathbf{grad} x_w^{NaCl} \right\} = q^s, \quad (A3)$$

- where Eq. A2 is the total mole balance of brine and Eq. A3 is the transport equation for NaCl. Further neglecting the effects of variable-density flow due to salt transport leads to a single-phase, single-component model (1p1c) where salt is considered as a pseudo component which influences the brine viscosity and the density (similar to a constant geothermal gradient) but the salinity stays constant during the simulation.

<sup>1</sup><https://git.iws.uni-stuttgart.de/dumux-pub/Kissinger2016a.git>

<sup>2</sup>[www.dumux.org](http://www.dumux.org)



In all models the porosity is a function of pressure under the assumption of a constant compressibility:

$$\phi = \phi_{ref} \left( 1 + X + \frac{X^2}{2} \right), \quad X = C(p - p_{ref}). \quad (\text{A4})$$

Here  $\phi_{ref}$  is the reference porosity,  $C$  is the compressibility and  $p_{ref}$  is the reference or initial pressure. The equations of state used in the models are given in Table 3. For spatial discretization, the BOX-Method is used, which is a node-centered finite  
5 volume method based on a finite element grid, see Helmig (1997) for further reference. For temporal discretization, a fully implicit scheme is applied using the Newton method to handle the system of non-linear partial differential equations.

### Fault zone representation using discrete fracture model

We consider a fault zone with a width of 50 m, while the horizontal discretization length is about 300 m. Thus, representing the geometry of the fault zone accurately would require grid refinement over large areas which would blow up the computational  
10 costs. To avoid refinement the fault zone is modeled with a discrete fracture approach. The fractures are defined on the element faces which leads to a simplification of the geometry but avoids severe grid refinement. Nodes connected by a fracture consider both matrix and fracture flow. Fracture flow only comprises advective flow (no diffusive flow) using a two-point flux approximation. Storage in the fracture is considered with an additional storage term for nodes connected to a fracture. A fracture can be described by three parameters: fracture width, fracture permeability and fracture porosity. The position of the fault zone is  
15 illustrated in the schematic shown in Fig. 7 marked in red.

#### Author contributions.

Holger Class and Alexander Kissinger	Numerical modeling
Stefan Knopf and Vera Noack	Geological expertise and geological model setup
Wilfried Konrad and Dirk Scheer	Participatory modeling

*Acknowledgements.* This study is part of the CO2BRIM research project. A major goal of the project is introducing participatory modeling in a joint engineering and social science approach as a means to involve potential stakeholders of CO<sub>2</sub> storage applications into the technical  
20 modeling process. The authors gratefully acknowledge the funding for the CO2BRIM project (03G0802A) provided by the German Federal Ministry of Education and Research (BMBF) and the German Research Foundation (DFG) within the geoscientific research and development program Geotechnologien.

Additionally, we would like to thank Christoph Jahnke for fruitful discussions and very helpful advice.



## References

- Adams, J. J. and Bachu, S.: Equations of state for basin geofluids: algorithm review and intercomparison for brines, *Geofluids*, 2, 257–271, doi:10.1046/j.1468-8123.2002.00041.x, <http://doi.wiley.com/10.1046/j.1468-8123.2002.00041.x>, 2002.
- Asprion, U., Griffel, G., and Elbracht, J.: Die neue Quartärbasis im deutschen Nordseesektor und im Küstenbereich der deutschen Nordsee.,  
5 Tech. rep., Landesamt für Bergbau, Energie und Geologie, Hannover, 2013.
- Batzle, M. and Wang, Z.: Seismic properties of pore fluids, *Geophysics*, 57, 1396, doi:10.1190/1.1443207, <http://library.seg.org/doi/abs/10.1190/1.1443207>, 1992.
- Birkholzer, J. T. and Zhou, Q.: Basin-scale hydrogeologic impacts of CO<sub>2</sub> storage: Capacity and regulatory implications, *International Journal of Greenhouse Gas Control*, 3, 745–756, doi:10.1016/j.ijggc.2009.07.002, <http://linkinghub.elsevier.com/retrieve/pii/S1750583609000668>,  
10 S1750583609000668, 2009.
- Birkholzer, J. T., Zhou, Q., and Tsang, C.-F.: Large-scale impact of CO<sub>2</sub> storage in deep saline aquifers: A sensitivity study on pressure response in stratified systems, *International Journal of Greenhouse Gas Control*, 3, 181–194, doi:10.1016/j.ijggc.2008.08.002, <http://linkinghub.elsevier.com/retrieve/pii/S1750583608000753>, 2009.
- Birkholzer, J. T., Cihan, A., and Zhou, Q.: Impact-driven pressure management via targeted brine extraction—Conceptual studies of  
15 CO<sub>2</sub> storage in saline formations, *International Journal of Greenhouse Gas Control*, 7, 168–180, doi:10.1016/j.ijggc.2012.01.001, <http://linkinghub.elsevier.com/retrieve/pii/S1750583612000023>, 2012.
- Bombien, H., Hoffers, B., Breuckmann, S., Helms, M., Lademann, K., Lange, M., Oelrich, A., Reimann, R., Rienäcker, J., and Schmidt, K.: Der Geotektonische Atlas von Niedersachsen und dem deutschen Nordseesektor als geologisches 3D-Modell, Tech. rep., 2012.
- Bots, P. W. G. and Daalen, C. E.: Participatory Model Construction and Model Use in Natural Resource Management: a Framework for  
20 Reflection, *Systemic Practice and Action Research*, 21, 389–407, doi:10.1007/s11213-008-9108-6, 2008.
- Brooks, R. J. and Corey, A. T.: Hydraulic properties of porous media, 1964.
- Celia, M. A. and Nordbotten, J. M.: Practical modeling approaches for geological storage of carbon dioxide, *Ground Water*, 47, 627–638, doi:10.1111/j.1745-6584.2009.00590.x, 2009.
- Celia, M. A., Nordbotten, J. M., Court, B., Dobossy, M., and Bachu, S.: Field-scale application of a semi-analytical model for estimation of  
25 CO<sub>2</sub> and brine leakage along old wells, *International Journal of Greenhouse Gas Control*, 5, 257–269, doi:10.1016/j.ijggc.2010.10.005, <http://dx.doi.org/10.1016/j.ijggc.2010.10.005>, 2011.
- Cihan, A., Zhou, Q., and Birkholzer, J. T.: Analytical solutions for pressure perturbation and fluid leakage through aquitards and wells in multilayered-aquifer systems, *Water Resources Research*, 47, doi:10.1029/2011WR010721, <http://doi.wiley.com/10.1029/2011WR010721>, 2011.
- 30 Cihan, A., Birkholzer, J. T., and Zhou, Q.: Pressure buildup and brine migration during CO<sub>2</sub> storage in multilayered aquifers., *Ground water*, 51, 252–67, doi:10.1111/j.1745-6584.2012.00972.x, <http://www.ncbi.nlm.nih.gov/pubmed/22880722>, 2013.
- Class, H., Ebigo, A., Helmig, R., Dahle, H. K., Nordbotten, J. M., Celia, M. A., Audigane, P., Darcis, M., Ennis-King, J., Fan, Y., Flemisch, B., Gasda, S. E., Jin, M., Krug, S., Labregere, D., Naderi Beni, A., Pawar, R. J., Sbai, A., Thomas, S. G., Trenty, L., and Wei, L.: A benchmark study on problems related to CO<sub>2</sub> storage in geologic formations, *Computational Geosciences*, 13, 409–434, doi:10.1007/s10596-  
35 009-9146-x, <http://link.springer.com/10.1007/s10596-009-9146-x>, 2009.
- Doornenbal, J. and Stevenson, A.: (Eds.) *Petroleum Geological Atlas of the Southern Permian Basin Area*, EAGE Publications b.v., Houten, 2010.



- Dreyer, M. and Renn, O.: Participatory approaches to modelling for improved learning and decision-making in natural resource governance: An editorial, *Environmental Policy and Governance*, 21, 379–385, doi:10.1002/eet.584, 2011.
- Dreyer, M., Konrad, W., and Scheer, D.: Partizipative Modellierung, in: *Methoden der Experten- und Stakeholdereinbindung in der sozialwissenschaftlichen Forschung*, edited by Niederberger, M. and Wassermann, S., pp. 265–289, Springer VS, Wiesbaden, 2015.
- 5 Fenghour, A., Wakeham, W. A., and Vesovic, V.: The Viscosity of Carbon Dioxide, *Journal of Physical and Chemical Reference Data*, 27, 31, doi:10.1063/1.556013, <http://link.aip.org/link/JPCRBU/v27/i1/p31/s1{&}Agg=doi>, 1998.
- Flemisch, B., Darcis, M., Erbertseder, K., Faigle, B., Mosthaf, K., Lauser, A., Müthing, S., Nuske, P., Tatomir, A., Wolf, M., and Helmig, R.: DUMUX: DUNE for multi-{phase, component, scale, physics, ...} flow and transport in porous media., *Advances in Water Resources*, 34, 1102–1112, doi:10.1016/j.advwaters.2011.03.007, 2011.
- 10 Fouché, C. and Light, G.: An invitation to dialogue ‘the world caf{é}’ in social work research, *Qualitative Social Work*, 10, 28–48, 2011.
- Helmig, R.: *Multiphase flow and transport processes in the subsurface: A contribution to the modeling of hydrosystems*, Springer, 1997.
- Huang, X., Bandilla, K. W., Celia, M. A., and Bachu, S.: Basin-scale modeling of CO<sub>2</sub> storage using models of varying complexity, *International Journal of Greenhouse Gas Control*, 20, 73–86, doi:10.1016/j.ijggc.2013.11.004, <http://linkinghub.elsevier.com/retrieve/pii/S1750583613003885>, 2014.
- 15 IEA (International Energy Agency): *Technology Roadmap Carbon Capture and Storage*, 2013.
- Jähne-Klingberg, F., Wolf, M., Steuer, S., Bense, F., Kaufmann, D., and Weitkamp, A.: *Speicherpotenziale im zentralen deutschen Nordsee-Sektor. - Technical report*, Bundesanstalt für Geowissenschaften und Rohstoffe, Hannover, 2014.
- Kaiser, B. O., Cacace, M., and Scheck-Wenderoth, M.: Quaternary channels within the Northeast German Basin and their relevance on Double Diffusive Convective transport processes: Constraints from 3D thermohaline numerical simulations, *Geochemistry, Geophysics, Geosystems*, pp. n/a–n/a, doi:10.1002/ggge.20192, <http://doi.wiley.com/10.1002/ggge.20192>, 2013.
- 20 Kaufmann, D., Heim, S., Jähne, F., Steuer, S., Bebiolka, A., Wolf, M., and Kuhlmann, G.: GSN – Generalisiertes, erweitertes Strukturmodell des zentralen deutschen Nordsee-Sektors – Konzept zur Erstellung einer konsistenten Datengrundlage für weiterführende Modellierungen im Bereich des zentralen deutschen Nordsee-Sektors, *Tech. rep.*, Bundesanstalt für Geowissenschaften und Rohstoffe, Hannover, 2014.
- Kempka, T., Herd, R., Huenges, E., Jahnke, C., Janetz, S., Jolie, E., Kühn, M., Magri, F., Möller, M., Munoz, G., Ritter, O., Schafrik, W., Schmidt-Hattenberger, C., Tillner, E., Voigt, H. J., and Zimmermann, G.: *brine: CO<sub>2</sub> - Speicherung in Ostbrandenburg: Implikationen für eine synergetische geothermische Energiegewinnung und Konzeptionierung eines Frühwarnsystems gegen Grundwasserversalzung*, *Tech. rep.*, 2013.
- 25 Knopf, S., May, F., Müller, C., and Gerling, P.: Neuberechnung möglicher Kapazitäten zur CO<sub>2</sub>-Speicherung in tiefen Aquifer-Strukturen, *Energiewirtschaftliche Tagesfragen*, 60, 76–80, 2010.
- 30 Larue, J.: *Endlagerung im Tonstein, Entwicklung eines synthetischen Tonsteinstandortes, Teil 2: Standortcharakterisierung. Abschlussberichte zum Vorhaben 3607R02538 „planerische Grundsatzfragen“*, *Tech. rep.*, GRS-A-3535, Köln, 2010.
- LBEG (Landesamt für Bergbau, Energie und Geologie): *CO<sub>2</sub>-Speicherung*, [http://www.lbeg.niedersachsen.de/energie\\_rohstoffe/co2speicherung/co2-speicherung-935.html](http://www.lbeg.niedersachsen.de/energie_rohstoffe/co2speicherung/co2-speicherung-935.html), 2012.
- LUGV (Landesamt für Umwelt, Gesundheit und Verbraucherschutz): *Hydroisohypsen des oberen genutzten Grundwasserleiters des Landes Brandenburg für das Frühjahr 2011, Daten des LUGV Brandenburg*, <http://www.mlul.brandenburg.de/cms/detail.php/bb1.c.310481.de>, accessed September 2014, 2012.
- 35 LUGV (Landesamt für Umwelt, Gesundheit und Verbraucherschutz): *Gewässernetz im Land Brandenburg [gwnet25\_\*.shp] Version 4.0. - Daten des LUGV Brandenburg*, <http://www.mlul.brandenburg.de/cms/detail.php/bb1.c.310481.de>, accessed September 2014, 2014.



- Magri, F., Bayer, U., Maiwald, U., Otto, R., and Thomson, C.: Impact of transition zones, variable fluid viscosity and anthropogenic activities on coupled fluid-transport processes in a shallow salt-dome environment, *Geofluids*, 9, 182–194, doi:10.1111/j.1468-8123.2009.00242.x, <http://doi.wiley.com/10.1111/j.1468-8123.2009.00242.x>, 2009a.
- Magri, F., Bayer, U., Pekdeger, A., Otto, R., Thomsen, C., and Maiwald, U.: Salty groundwater flow in the shallow and deep aquifer systems of the Schleswig-Holstein area (North German Basin), *Tectonophysics*, 470, 183–194, doi:10.1016/j.tecto.2008.04.019, <http://linkinghub.elsevier.com/retrieve/pii/S0040195108001790>, 2009b.
- Martens, S., Kempka, T., Liebscher, A., Lüth, S., Möller, F., Myrntinen, A., Norden, B., Schmidt-Hattenberger, C., Zimmer, M., and Kühn, M.: Europe's longest-operating on-shore CO<sub>2</sub> storage site at Ketzin, Germany: A progress report after three years of injection, *Environmental Earth Sciences*, 67, 323–334, doi:10.1007/s12665-012-1672-5, 2012.
- 10 Noack, V., Scheck-Wenderoth, M., Cacace, M., and Schneider, M.: Influence of fluid flow on the regional thermal field: results from 3D numerical modelling for the area of Brandenburg (North German Basin), *Environmental Earth Sciences*, 70, 3523–3544, doi:10.1007/s12665-013-2438-4, <http://link.springer.com/10.1007/s12665-013-2438-4>, 2013.
- Nordbotten, J., Flemisch, B., Gasda, S., Nilsen, H., Fan, Y., Pickup, G., Wiese, B., Celia, M., Dahle, H., Eigestad, G., and Pruess, K.: Uncertainties in practical simulation of CO<sub>2</sub> storage, *International Journal of Greenhouse Gas Control*, 9, 234–242, doi:10.1016/j.ijggc.2012.03.007, <http://linkinghub.elsevier.com/retrieve/pii/S1750583612000655>, 2012.
- 15 Nordbotten, J. M., Kavetski, D., Celia, M. a., and Bachu, S.: Model for CO<sub>2</sub> leakage including multiple geological layers and multiple leaky wells., *Environmental science & technology*, 43, 743–9, <http://www.ncbi.nlm.nih.gov/pubmed/19245011>, 2009.
- Oldenburg, C. M. and Rinaldi, A. P.: Buoyancy Effects on Upward Brine Displacement Caused by CO<sub>2</sub> Injection, *Transport in Porous Media*, 87, 525–540, doi:10.1007/s11242-010-9699-0, <http://link.springer.com/10.1007/s11242-010-9699-0>, 2010.
- 20 Reinhold, K., Krull, P., and Kockel, F.: Salzstrukturen Norddeutschlands 1:500 000. Bundesanstalt für Geowissenschaften und Rohstoffe, Berlin/Hannover, 2008.
- Reinhold, K., Müller, C., and Riesenberger, C.: Informationssystem Speichergesteine für den Standort Deutschland - Synthese -, Tech. rep., Bundesanstalt für Geowissenschaften und Rohstoffe (BGR), Hannover, 2011.
- Reutter, E.: Hydrostratigrafische Gliederung Niedersachsens, *Geofakten*, 21, 2011.
- 25 Röckmann, C., Ulrich, C., Dreyer, M., Bell, E., Borodzic, E., Haapasaari, P., Hauge, K. H., Howell, D., Mäntyniemi, S., Miller, D., Tserpes, G., and Pastoors, M.: The added value of participatory modelling in fisheries management - what has been learnt?, *Marine Policy*, 36, 1072–1085, doi:10.1016/j.marpol.2012.02.027, 2012.
- Schäfer, F., Walter, L., Class, H., and Müller, C.: The regional pressure impact of CO<sub>2</sub> storage: a showcase study from the North German Basin, *Environmental Earth Sciences*, 65, 2037–2049, doi:10.1007/s12665-011-1184-8, <http://www.springerlink.com/index/10.1007/s12665-011-1184-8>, 2011.
- 30 Scheer, D., Konrad, W., Class, H., Kissinger, A., Knopf, S., and Noack, V.: Expert involvement in science development: (re-)evaluation of an early screening tool for carbon storage site characterization, *International Journal of Greenhouse Gas Control*, 37, 228–236, doi:10.1016/j.ijggc.2015.03.023, <http://linkinghub.elsevier.com/retrieve/pii/S1750583615001152>, 2015.
- Schrader, C.: 13. October 2014. Expressfahrstuhl für Salzwasser, *Süddeutsche Zeitung*, p. 16.
- 35 Schulz, R., Suchi, E., Öhlschläger, D., Dittmann, J., Knopf, S., and Müller, C.: Geothermie-Atlas zur Darstellung möglicher Nutzungskonkurrenzen zwischen CCS und Tiefer Geothermie, Tech. rep., LIAG-Bericht, Archiv-Nr. 131 310: 108 S., Hannover, 2013.





- Schwenck, N., Beck, M., Becker, B., Class, H., Fetzer, T., Flemisch, B., Grüninger, C., Hommel, J., Jambhekar, V., Kissinger, A., Koch, T., Schneider, M., Schröder, N., Seitz, G., and Weishaupt, K.: DuMuX 2.8.0, doi:10.5281/zenodo.31611, <http://dx.doi.org/10.5281/zenodo.31611>, 2015.
- Skalmaraas, O.: The Sleipner CCS experience, in: United Nations Framework Convention on Climate Change, Bonn, October 21., 2014.
- 5 Span, R. and Wagner, W.: A New Equation of State for Carbon Dioxide Covering the Fluid Region from the Triple-Point Temperature to 1100 K at Pressures up to 800 MPa, *Journal of Physical and Chemical Reference Data*, 25, 1509, doi:10.1063/1.555991, <http://link.aip.org/link/JPCRBU/v25/i6/p1509/s1>{&}Agg=doi, 1996.
- Tillner, E., Kempka, T., Nakaten, B., and Kühn, M.: Brine migration through fault zones: 3D numerical simulations for a prospective CO<sub>2</sub> storage site in Northeast Germany, *International Journal of Greenhouse Gas Control*, doi:10.1016/j.ijggc.2013.03.012, <http://linkinghub.elsevier.com/retrieve/pii/S1750583613001321>, 2013.
- 10 Walter, L., Binning, P. J., Oladyshkin, S., Flemisch, B., and Class, H.: Brine migration resulting from CO<sub>2</sub> injection into saline aquifers - An approach to risk estimation including various levels of uncertainty, *International Journal of Greenhouse Gas Control*, 9, 495–506, doi:10.1016/j.ijggc.2012.05.004, 2012.
- Walter, L., Binning, P. J., and Class, H.: Predicting salt intrusion into freshwater aquifers resulting from CO<sub>2</sub> injection – A study on the influence of conservative assumptions, *Advances in Water Resources*, 62, 543–554, doi:10.1016/j.advwatres.2013.09.017, <http://linkinghub.elsevier.com/retrieve/pii/S0309170813001784>, 2013.
- Wolf, M., Steuer, S., Jähne, F., Kaufmann, D., and Weitkamp, A.: 3D-Lithofaziesmodell des Buntsandstein in der zentralen deutschen Nordsee, Tech. rep., Bundesanstalt für Geowissenschaften und Rohstoffe, Hannover, 2014.
- Zeidouni, M.: Analytical model of leakage through fault to overlying formations, *Water Resources Research*, 48, n/a–n/a, doi:10.1029/2012WR012582, <http://doi.wiley.com/10.1029/2012WR012582>, 2012.
- 20